fermentation

MDPI

Article

Simultaneous Saccharification and Fermentation of Empty Fruit Bunches of Palm for Bioethanol Production Using a Microbial Consortium of *S. cerevisiae* and *T. harzianum*

Eryati Derman [1], Rahmath Abdulla [1,*], Hartinie Marbawi [1], Mohd Khalizan Sabullah [1], Jualang Azlan Gansau [1] and Pogaku Ravindra [2]

[1] Faculty of Science and Natural Resources, University Malaysia Sabah, Kota Kinabalu 88400, Malaysia; eryatiderman@gmail.com (E.D.); hartinie@ums.edu.my (H.M.); khalizan@ums.edu.my (M.K.S.); azlanajg@ums.edu.my (J.A.G.)

[2] Chemical and Bioprocess Engineering, Rowan University, Glassboro, NJ 08322, USA; dr_ravindra@hotmail.com

* Correspondence: rahmath@ums.edu.my; Tel.: +60-8-832-0000 (ext. 5592)

Abstract: A simultaneous saccharification and fermentation (SSF) optimization process was carried out on pretreated empty fruit bunches (EFBs) by employing the Response Surface Methodology (RSM). EFBs were treated using sequential acid-alkali pretreatment and analyzed physically by a scanning electron microscope (SEM). The findings revealed that the pretreatment had changed the morphology and the EFBs' structure. Then, the optimum combination of enzymes and microbes for bioethanol production was screened. Results showed that the combination of *S. cerevisiae* and *T. harzianum* and enzymes (cellulase and β-glucosidase) produced the highest bioethanol concentration with 11.76 g/L and a bioethanol yield of 0.29 g/g EFB using 4% (*w/v*) treated EFBs at 30 °C for 72 h. Next, the central composite design (CCD) of RSM was employed to optimize the SSF parameters of fermentation time, temperature, pH, and inoculum concentration for higher yield. The analysis of optimization by CCD predicted that 9.72 g/L of bioethanol (0.46 g/g ethanol yield, 90.63% conversion efficiency) could be obtained at 72 h, 30 °C, pH 4.8, and 6.79% (*v/v*) of inoculum concentration using 2% (*w/v*) treated EFBs. Results showed that the fermentation process conducted using the optimized conditions produced 9.65 g/L of bioethanol, 0.46 g/g ethanol yield, and 89.56% conversion efficiency, which was in close proximity to the predicted CCD model.

Keywords: empty fruit bunches; response surface methodology; central composite design; simultaneous saccharification and fermentation; bioethanol

Citation: Derman, E.; Abdulla, R.; Marbawi, H.; Sabullah, M.K.; Gansau, J.A.; Ravindra, P. Simultaneous Saccharification and Fermentation of Empty Fruit Bunches of Palm for Bioethanol Production Using a Microbial Consortium of *S. cerevisiae* and *T. harzianum*. *Fermentation* **2022**, *8*, 295. https://doi.org/10.3390/fermentation8070295

Academic Editor: Alessia Tropea

Received: 12 May 2022
Accepted: 9 June 2022
Published: 23 June 2022

1. Introduction

Biofuel has attracted lots of attention among renewable energy resources due to its potential to replace existing fossil fuels in order to alleviate the global energy crisis and its demand [1]. This awareness has led to a dramatic increase in biofuel production and research [2]. Sustainable and renewable liquid biofuels such as bioethanol are seen as an alternative to fossil gasoline substitution and replacement [3]. Bioethanol is considered a natural and ecological fuel, can be produced from renewable energy sources, and is widely used in automobile engines [4,5]. This can be done mainly by reducing the operational cost as well as using cheaper and sustainable feedstocks [6]. Thus, research on bioethanol production using renewable, sustainable, and non-food feedstock is important to overcome the issue of fossil fuel demand.

Empty fruit bunches (EFBs) are cheap, readily available, and accessible biomass wastes in the oil palm industries in Malaysia [7–9]. Recently, they emerged as a potential biomass feedstock in producing bioethanol because of their great abundance and favorable physiochemical characteristics [10,11]. Three important components in EFBs, such as

lignin, hemicellulose, and cellulose, make it possible for the EFBs to be converted into bioethanol [12,13]. However, an in-depth study into the bioconversion process is needed to fully utilize EFBs for bioethanol production. An efficient bioconversion process of EFBs into bioethanol is crucial as it affects the ethanol yield and also the overall cost of bioethanol production [8,14]. One of the strategies to reduce the production cost is by operating the fermentation process at a high loading substrate and low enzyme requirement [15].

Bioethanol production from EFBs can be carried out in two ways, which are the separate hydrolysis and fermentation (SHF) and simultaneous saccharification and fermentation (SSF) processes. However, SSF is preferred over SHF as the whole process of SSF is performed in a single vessel combining both processes of hydrolysis and fermentation to produce bioethanol [16,17]. This helps in reducing the chances of contamination in the fermentation medium that occur during SHF [18]. Moreover, this process is a fitting technique for the production of bioethanol, as sugars formed from biomass are rapidly converted into bioethanol at higher concentrations and yields [19,20]. Thus, diminishing the accumulation of inhibitory sugars, end-product inhibition and bioethanol presence in the medium will also make it less vulnerable to contamination [21,22]. In the SSF process, both enzymes and microorganisms are used at the same time. Hence, the optimization of process parameters should be investigated to obtain the maximum amount of sugars that can be converted to bioethanol during the process of saccharification [23]. For example, the optimal conditions for hydrolysis using cellulolytic enzymes is between 40 °C and 50 °C, but microorganisms for fermentation work best around 30 °C and 40 °C [24–26]. Therefore, it is important to strike a balance between the optimal conditions for the enzymes and microorganisms used in the SSF process. Choosing an ideal EFB bioconversion process into bioethanol is also very important to establish optimal fermentation conditions for both enzymes and microorganisms in order to develop a cost-efficient bioethanol production.

In this study, a microbial consortium of *S. cerevisiae* and *T. harzianum* were used in the simultaneous saccharification and fermentation (SSF) process of EFBs. A microbial consortium was used in the SSF process instead of using a single microbe, as it not only utilizes substrate more efficiently but also increases the product yield [23]. In a study by Polprasert et al. [27], palm EFBs were used as a substrate to produce ethanol using a microbial consortium of *Saccharomyces cerevisiae* and *Pichia stipitis* at a 1:1 ratio for bioethanol production. In another study conducted by Ali et al. [28], it is highlighted that higher bioethanol production from date palm fronds was achieved by using the same microbial consortium of *S. cerevisiae* and *P. stipitis*. Mishra and Ghosh [29] reported that the maximum theoretical ethanol production from Kans grass biomass was achieved at 78.6% with 0.45 g/g ethanol yield by using a microbial consortium of *Zymomonas mobilis* and *Scheffersomyces shehatae*. Similarly, Izmirlioglu and Demirci [30] produced 35.19 g/L ethanol from 92.37 g/L industrial waste potato mash, which corresponds to 0.38 g ethanol/g starch when *Aspergillus niger* and *S. cerevisiae* co-cultured in the fermentation process. Kabbashi et al. [31] compared the compatibility of several fungi and yeast to develop direct solid-state bioconversion using the potential mixed culture to produce bioethanol. From the study, the mixed culture of a fungus (*T. harzianum*) and a yeast (*S.cerevisiae*) showed the best ethanol production with 14.1% (*v*/*v*) bioethanol concentration compared to other mixed culture combinations, which produced bioethanol concentrations in the range of 6.4 to 7.5% (*v*/*v*). At present, finding ideal optimization parameters for the simultaneous saccharification and fermentation process for all the concerned microbial strains and enzymes are important to enhance the utilization of substrate and increase the ethanol production yield.

To the best of the authors' knowledge, there has been no published optimization study for the fermentation process using RSM for bioethanol production from EFBs employing a mixed microbial consortium. Meanwhile, the SSF process using microbial strains had been well studied using a wide range of lignocellulosic biomass, but reports on using a microbial consortium for EFB fermentation are limited. Therefore, the aim of this study is to optimize the production of bioethanol using a microbial consortium of *S. cerevisiae* and *T. harzianum* during the simultaneous saccharification and fermentation (SSF) process of

EFBs by employing the central composite design (CCD) of Response Surface Methodology (RSM). The employment of CCD for optimization would benefit researchers, as by using this design, the expensive cost of the analysis could be reduced as it provides a large amount of information from a few experimental runs. RSM is also able to overcome the limitation of one-at-a-time parameter optimization.

2. Materials and Methods

2.1. Raw Materials

Empty fruit bunches (EFBs) were provided by a local palm oil processing mill in Beaufort, Sabah (Lumadan Palm oil Mill). The collected samples in the form of whole bunches were initially shredded before washing with tap water to remove salts, dirt, oil, and debris. Then, the EFBs were dried at 70 °C for 72 h to remove residual moisture until a constant weight was obtained. They were then blended using a laboratory blender (Waring Commercial), sieved, and separated into fractions using a test sieve [32]. The particle size of EFBs used for this study is 0.1–0.5 mm to maximize the contact area of the substrate and to facilitate the pretreatment and enzymatic hydrolysis process [19,27]. The samples were stored in sealed plastic bags and in a dry place until further use.

2.2. Chemicals and Microorganisms

The enzymes cellulase (cellulase from Trichoderma reesei ATCC 26921, aqueous solution, 50 mL) and β-glucosidase (EC 3.2.1.21 from almonds, 0.88 g solid, crude, lyophilized powder) were purchased from Sigma Aldrich, St. Louis, MO, USA. The cellulase had an activity of 700 units/g while the β-glucosidase had an activity of 2.85 units/mg solid. The enzymes, cellulase and β-glucosidase, were used in the saccharification process. The yeast strain *Saccharomyces cerevisiae* Type II (YSCII) and fungi strain *Trichoderma harzianum* W2(4)-1(2) were employed for this research. Yeast from Saccharomyces cerevisiae Type II (YSII) was purchased from Sigma Aldrich, USA. *Trichoderma harzianum* was supplied by Dr. Syafiquezzaman from the Biotechnology Research Institute, UMS.

Microorganisms Cultivation

Saccharomyces cerevisiae Type II (YSII) and *Trichoderma harzianum* W2(4)-1(2) were used as an ethanol fermentation strain. Both the yeast and fungi strains were cultured in potato dextrose agar (PDA) at 30 °C, which was then maintained and stored at 4 °C until further use [33]. In this study, the growth rates of the *S. cerevisiae*, *T. harzianum*, and co-culture of *S. cerevisiae* and *T. harzianum* were evaluated by measuring the optical densities (OD) at a wavelength of 600 nm [34]. The approximate number of cells in the culture can be determined with a spectrophotometer by measuring the optical density (OD) at 600 nm [35] every three hours for 48 h using a microplate reader (Multiskan go, Thermo Scientific) to identify the growth phases of both microorganisms. A growth curve was drawn based on the OD_{600} measured.

Then, the fermentation inoculums were prepared by inoculating a loopful of the microbial consortium of *S. cerevisiae* and *T. harzianum* cells into a 50 mL sterile potato dextrose broth (PDB) medium and harvested at the exponential phase [36]. At the exponential growth of co-cultured *S. cerevisiae* and *T. harzianum*, the active cells were centrifuged in a refrigerated centrifuge (10,000 rpm at 4 °C for 10 min), washed with sterile distilled water three times, and then the precipitated cells were collected under aseptic conditions and added to the fermentation stage as inoculums [37,38].

2.3. Pretreatments of EFBs

Dried EFBs were soaked in 2% (*v*/*v*) sulphuric acid (H_2SO_4) and incubated in an autoclave at 121 °C, 15 psi for 20 min. The dilute acid-treated EFBs fibers were then soaked in water and occasionally mixed for 1 h [25]. The washed EFBs were then dried at 70 °C overnight. The dried acid-treated EFBs were soaked in 10% (*w*/*v*) sodium hydroxide (NaOH) solution [39,40], stirred at ambient temperature for 4 h, and then recovered from

the alkali solution. The EFBs in the wet alkali solid-state were heated again at 121 °C, 15 psi, for 20 min. The thermal-treated biomass was soaked in the water and stirred occasionally to remove NaOH from the surface. The samples were washed several times with distilled water to neutralize the pH, after which they were dried in an oven at 70 °C overnight [25]. The pretreated EFBs were then stored in a sealed plastic bag until further use.

2.4. EFBs Analysis

2.4.1. Scanning Electron Microscope (SEM) Analysis of EFBs

The untreated and pretreated EFBs were subjected to microscopic observation. The samples were washed with distilled water before drying at 70 °C for 24 h [32]. The dried samples were subjected to SEM using a Carl Zeiss MA10 model brand which has elemental analysis and chemical characterization with element surface mapping via EDX (Energy Dispersive X-ray Spectroscopy). The EFB samples were mounted on conductive tape and coated with gold particles prior to analysis.

2.4.2. Fourier Transform Infrared (FTIR) Analysis of EFBs

FTIR analysis was performed to evaluate the infrared spectrum that shows the chemical composition of the samples. The difference between the untreated and pretreated EFBs was studied using FTIR analysis (Perkin Elmer). The spectra for the samples were recorded in the wavelength range of 400 to 4000 cm^{-1} with the direct transmittance at the rate of 4 scans/min [41]. The FTIR spectra were smoothened and corrected to the baseline correction. The formation, breaking, and shifting of bands were observed. Functional groups associated with major vibration bands were also determined.

2.5. Enzymatic Saccharification of EFBs

The enzymatic saccharification of the acid/alkali pretreated EFBs was performed using cellulase derived from *Trichoderma reesei* (*Trichoderma reesei* ATCC 26921) and β-glucosidase (EC 3.2.1.21 from almonds). The amount of enzyme used was 50 U/g of cellulase and 10 U/g of β-glucosidase. The pretreated EFBs of 4% (*w*/*v*) were hydrolyzed in a 50 mM citrate buffer (pH 4.8). The samples were then incubated at 50 °C, 150 rpm, for 72 h. Sample aliquots were withdrawn at 24 h intervals and analyzed for reducing sugar glucose [32].

2.6. Selection of Microorganisms and Enzyme Combinations

In this study, the combination of microorganisms of *S. cerevisiae* and *T. harzianum* and also the combination of cellulase from T. reesei and β-glucosidase from almonds were employed for the simultaneous saccharification and fermentation (SSF) process. The selection was done to determine which combination can enhance the conversion of EFBs into ethanol during the fermentation process. Different microorganism and enzyme combinations (Table 1) at constant inoculum loadings of the microorganisms at 10% (*v*/*v*)—50 U/g for cellulase and 10 U/g for β-glucosidase—were added under baseline parameters of 4% (*w*/*v*) of pretreated empty fruit bunches at a fixed volume (50 mL) of sodium citrate buffer (pH 4.8) at a temperature of 30 °C for 72 h in a 250 mL Erlenmeyer flask and placed in an orbital shaker (Heidolph Incubator 1000) operated at an agitation speed of 150 rpm (triplicates for each run). After 72 h of fermentation time, the fermentation product was immediately heated for 5 min in a boiling water bath to end the enzymatic reaction. The fermentation product was then centrifuged (Thermo Scientific, Heraeus Megafuge 16R) at 10,000 rpm for 10 min. The supernatant was taken and used in the distillation process to obtain the ethanol. Then, the ethanol produced was subjected to ethanol analysis using gas chromatography–mass spectrometry (GC–MS). The combination which produced the higher ethanol concentration was selected for the fermentation process.

Table 1. Different combinations of microorganisms (*S. cerevisiae* and *T. harzianum*) and enzymes (Cellulase and β-glucosidase).

Combination	Microorganisms and Enzymes			
	S. cerevisiae	*T. harzianum*	Cellulase	β-glucosidase
M1	✓	✓	✓	✓
M2	✓	✓	✓	
M3	✓	✓		✓
M4		✓	✓	✓
M5		✓	✓	
M6	✓	✓		✓
M7	✓		✓	✓
M8	✓		✓	
M9	✓			✓

Operating conditions: 4% (*w*/*v*) pretreated EFBs, at constant inoculums loading of 10% (*v*/*v*) for each combination, pH 4.8, temperature 30 °C, for 72 h at 150 rpm.

2.7. Optimization of Simultaneous Saccharification and Fermentation

The statistical analysis of Response Surface Methodology (RSM) was utilized to optimize the simultaneous saccharification and fermentation process by employing the central composite design (CCD). Various parameters or factors affecting the SSF process of EFBs for bioethanol production were optimized.

Central Composite Design (CCD) for Optimization

The CCD of RSM was applied to determine the optimum conditions of the significant parameters for the SSF process. The effect of fermentation time (24–72 h), temperature (30–50 °C), pH (4.8–6.0), and inoculum concentration (5–10% *v*/*v*) on the production of bioethanol were studied at five experimental levels (−2 (α), −1, 0, +1, +2 (α)). The design matrix of 30 sets of experimental runs was generated from the CCD of RSM software. All the 30 experiments with three replicates were carried out according to the design matrix to screen the best optimum value of each parameter for bioethanol production [42]. The response surface graphs were obtained using the software to understand the effect of variables individually and in combination, in order to determine their optimum levels.

The experimental runs were carried out according to a 2^4 full factorial design for the four identified design independent variables with low (−1) and high (+) levels. The total number of experiments (runs) was given by the simple formula [$30 = 2^k + 2k + 6$], where k is the number of independent variables (k = 4); this includes the following: 16 factorial points from 24 full factorial CCDs were augmented with 6 replicates at the center point to assess the pure error. The response was selected based on preliminary study results. The design factors (variables) with low −1 and high +1 levels are, namely, A (24 and 72), B (30 and 50), C (4.8 and 6), and D (5 and 10). The central values (zero levels) chosen for experimental design were as follows: 48 h, 40 °C, pH 5.4, and 7.5 % (*v*/*v*) for A, B, C, and D, respectively (Table 2) [43].

Table 2. Experimental range and levels of variables used in the Central Composite Design for the optimization of fermentation.

	Parameters	Levels				
		−2 (α)	−1	0	+1	+2 (α)
A	Fermentation Time, (h)	0.0	24.0	48.0	72.0	96.0
B	Temperature, (°C)	20.0	30.0	40.0	50.0	60.0
C	pH	4.2	4.8	5.4	6.0	6.6
D	Inoculum concentration, % (*v*/*v*)	2.5	5.0	7.5	10.0	12.5

2.8. Simultaneous Saccharification and Fermentation

The simultaneous saccharification and fermentation of the acid-alkali-pretreated EFBs were performed in a fixed volume of 100 mL of citrate buffer broth (1% (*w*/*v*) yeast extract, 2% (*w*/*v*) peptone, and 4% (*w*/*v*) pretreated EFBs) in a 250 mL Erlenmeyer flask in an orbital incubator shaker (Heidolph, Uimax 1010 and Incubator 1000) at an agitation speed of 150 rpm. Combinations of different microorganisms (*S. cerevisiae* and *T. harzianum*) and enzymes (Cellulase and β-glucosidase) were used in the bioethanol fermentation. The sample obtained at the end of the fermentation process was centrifuged at 10,000 rpm for 10 min. The pellet was discarded and only the supernatant was transferred to the new Falcon tube. The fermenting products were then quantified for their bioethanol concentration after undergoing the distillation process to obtain the bioethanol.

2.9. Analytical Methods

2.9.1. Bioethanol Determination

The ethanol contents of the samples after the distillation process were analyzed using gas chromatography–mass spectrometry (GC–MS) (Model 6890N, Agilent Technologies, CA, USA) equipped with a thermal conductivity detector and an HP−5MS column, 0.25 mm × 30 m, 0.25 µm ID. Samples were filtered through a Durapore (PVDF) syringe-driven filter unit (0.2 µm) into 1.5 mL glass vials, sealed with a cap, and kept at 5–8 °C before being analyzed using GC–MS. The sample (1.0 µL) was injected into the GC–MS in split mode with a split ratio of 100:1. Helium gas with 99.995% purity was used as the carrier gas and its flow rate was set to 10.0 mL/min. The initial temperature of the oven was 40 °C and was increased at a rate of 10 °C/min up to 100 °C [44]. Hexane was used as the solvent for the standard and sample dilution.

2.9.2. Statistical Analysis of the Experiment

The bioethanol yield (g/g) was calculated based on the experiment and expressed as g of bioethanol per total g of glucose utilizing Equation (1) and g of bioethanol per total g of EFBs utilizing Equation (2). The bioethanol conversion efficiency or theoretical ethanol yield (%) was calculated based on the ratio of ethanol yield obtained against the theoretical maximum ethanol yield using Equation (3) [32,45].

$$\text{Bioethanol yield (g/g) of glucose} = \frac{\text{Bioethanol concentration (g/L)}}{\text{Initial glucose concentration (g/L)}} \quad (1)$$

$$\text{Bioethanol yield/g of EFBs} = \frac{\text{Bioethanol concentration (g/L)}}{\text{Substrate (EFBs) used (g)}} \quad (2)$$

$$\text{Conversion efficiency (\%)} = \frac{[\text{EtOH}]}{0.51} \times 100\% \quad (3)$$

3. Results and Discussion

3.1. Pretreatment of EFBs

The chemical composition of EFBs includes cellulose, hemicellulose, and lignin fractions. The approximate percentage compositions of EFBs depend on the source of the EFBs. Table 3 shows the chemical composition of EFBs from a previous study before and after the pretreatment process. It can be seen that cellulose has the highest content (%), followed by hemicelluloses, lignin, and ash. The amount of cellulose in EFB increases while the hemicellulose and lignin content decrease after the pretreatment process. The previous study by Burhani et al. [46] obtained 90.5% cellulose, no trace of hemicellulose, and 9.13% lignin after the pretreatment process. In a study by Campioni et al. [47], it was reported that there was an increase in EFB cellulose content after acid-alkali pretreatment from 42.2 to 62.6%. Different authors observed different EFB compositions obtained after the acid-alkali pretreatment process. Akhtar et al. [48] reported that in the first step of the pretreatment of

EFB using dilute acid, 90% of hemicellulose and 10% of lignin were removed and further treatment using dilute alkali with a microwave achieved 71.9% delignification.

The development of pretreatment is one of the crucial steps in bioethanol production to minimize the sugar loss, limit the inhibitor formation, and maximize the lignin removal [49]. Most of the hemicellulose contents of EFBs are usually lost after the acid-alkali pretreatment. A study by Kim and Kim [25] demonstrated that sequential acid-alkaline pretreatment efficiently reduced the hemicellulose and lignin content in EFBs. EFB biomass normally has 50 to 80% complex carbohydrates containing C6 and C5 sugar units. According to Abdul et al. [50], oil palm EFB fibers have about 60% (w/w) sugar components. However, no sugar loss was observed in the EFBs when they were pretreated using the ammonia fiber expansion (AFEX) method. In addition, Taherzadeh and Karimi [51], reported that the chemical pretreatment of lignocellulosic material should remove maximum lignin contents with no more than 5% sugar loss. In this work, the authors used a chemical acid agent, 2% (*v*/*v*) H_2SO_4, an alkaline agent, and 10% (*w*/*v*) NaOH solution.

Table 3. Chemical composition of EFBs before and after the pretreatment process.

	EFB Components	Content (%)				
Untreated	Cellulose	25.71	42.2	41.8	32.26	36.59
	Hemicellulose	17.37	29.4	35.6	17.62	24.97
	Lignin	34.02	13.8	18.8	33.02	26.53
	Ash	-	-	-	1.82	1.79
Treated	Cellulose	90.5	62.6	85.4	65.91	75.05
	Hemicellulose	0.00	5.6	3,5	15.55	10.19
	Lignin	9.13	24.3	5.3	11.70	8.11
	Ash	-	-		0.62	2.22
References		[46] [a]	[47] [a]	[48] [a]	[52] [b]	[53] [b]

The chemical composition of treated EFBs is based on the best result of the pretreatment process taken from the respective journal. [a] Sequential acid-alkaline pretreatment using H_2SO_4 and NaOH. [b] Alkaline pretreatment using NaOH.

The effects of sequential acid-alkali pretreatment on EFBs were measured by comparing the physical characteristics of the EFBs before and after pretreatment, shown in Figure 1. Moreover, changes in the EFBs' structure were also analyzed by using the scanning electron microscope (SEM) and Fourier Transform Infrared Spectroscopy (FTIR).

3.1.1. Physical Analysis of EFBs

The physical characteristics of the pretreated EFBs and the non-treated EFBs were observed and are presented in Figure 1. In general, the visual observation, which can be seen between the non-treated and treated EFBs, is the color and structure of the EFBs. From the figure, it can be seen that the surfaces of the non-treated EFB fibers (Figure 1a) have clear, well-ordered, and rigid fibrils, while the pretreated EFB fibers (Figure 1b) showed porous, rough, and irregularly ordered fibrils after the pretreatment process.

Morphological differences between the EFBs occurred due to the removal of the fibril components during the pretreatment process. Physical changes occurred on the surface of treated EFBs that enable easier enzyme access to hydrolyze the cellulose components into glucose and further facilitate the performance of enzymatic hydrolysis [54]. The treated EFBs also changed color to dark brown. This is due to an increase in steam temperature, which caused the degradation of carbohydrates when the EFBs were autoclaved at 121 °C [55]. Furthermore, the treated EFBs were more fragile compared to the non-treated EFBs.

(**a**) Non-treated EFBs

(**b**) Treated EFBs

Figure 1. Physical characteristics of the EFBs: (**a**) non-treated EFB fiber; (**b**) sequential acid/alkali-pretreated EFBs fiber.

The composition of biomass plays an important role in the pretreatment methods selection [56]. Musatto et al. [57] reported that the sequential acid-alkali pretreatment technique was used in order to eliminate the protective lignin-hemicellulose wrapper of the EFBs. The sequence of pretreatment in combined form gave a high impact on reducing sugar production by increasing the cellulose and reducing the hemicellulose and lignin content [58]. In the work performed by Campioni et al. [47], EFBs' cellulose content was increased from 42.2 to 62.6% after acid and alkali treatment, while their hemicellulose component had a mass loss of about 90% and a lignin loss of about 25%.

In the pretreatment process, chemical pretreatment using acid (low pH) and alkali (high pH) techniques can be used to boost the hydrolytic reactivity [59]. The acid pretreatment technique helps in the hydrolysis of hemicellulose fractions and lignin content reduction in biomass [60,61]. On the other hand, the alkaline pretreatment of lignocelluloses with NaOH can modify or remove lignin content in the feedstocks by fracturing the ester bonds, which are cross-links between lignin and xylan, so that the porosity of the biomass can be increased [40]. Furthermore, the alkali (NaOH) pretreatment technique is effective in exposing the cellulose to cellulose digestion by breaking the hemicelluloses–lignin linkage in the amorphous-crystalline structure of cellulose, thus enabling easier conversion of EFBs into glucose [62]. During pretreatment, NaOH penetrates and swells the substrate and solubilizes the hemicellulose, lignin, and the other non-cellulose components [63].

EFBs are usually incubated in an autoclave at 121 °C for 20 min to maximize the effect of NaOH and H_2SO_4 on lignin extraction [64]. Autoclaving at 121 °C and 15 psi is the best way to alter the chemical composition and physical structure of the EFBs, as well as increasing the reducing sugar production. High temperature promotes the removal of both hemicelluloses and lignin (delignification). Akhtar et al. [48] found that 90% of EFBs' hemicellulose was removed after the EFBs were soaked in dilute H_2SO_4 with additional autoclave heating. The combination of NaOH treatment at 10 MPa pressure and 121 °C during pretreatment disintegrated EFB fibers into pliable fibers. It also cleans up the fiber surface and thus exposes more cellulose components in the EFB fibers. Moreover, mass

losses of EFBs occur due to the heating of the EFBs at a high temperature when autoclaved at 121 °C, as this causes degradation in the EFBs' hemicelluloses and lignin contents [65].

3.1.2. Scanning Electron Microscope (SEM) Analysis of EFBs

The SEM analysis of EFBs was conducted in order to study the effects of the pretreatment process based on its microscopic morphology differences. A distinct change in the EFBs' physical appearance can be seen in the structure of the untreated EFBs in Figure 2a,b and treated EFBs in Figure 2c,d. In Figure 2a, the untreated sample structures are complete, compact, rigid, and have a smooth surface. This is because no pretreatment process was used to destruct the lignocellulose component of the EFBs [64,66]. According to Tye et al. [67], untreated biomass usually shows low enzymatic hydrolyzability because the enzyme accessibility is restricted by the recalcitrance polymer lignin and hemicellulose.

For the treated sample in Figure 2c, there is a formation of pores on the EFB surface. The presence of pores occurs due to the removal of hemicelluloses [58]. It was reported that the pretreated lignocellulose, which has fractions of pores, was more accessible for enzymatic attack [32]. This is because pretreatment effectively degraded and exposed more surface area of fermentable sugars for the enzymatic hydrolysis process [56]. Pores present in the EFBs are also thought to be effective in the swelling of the EFBs' structure, thus attracting the enzymatic and microbe reactions for the bioconversion process [55,68]. It is revealed that the sequential acid-alkali pretreatment process changed the morphology of the EFBs and gave the biggest impact on the alteration of the EFB structure by removing the silica, which is the chemical composition barrier, causing pore formation.

The SEM micrographs for non-treated EFB surfaces (Figure 2a,b) showed a silica body embedded on the surface. From the figure, it can be seen that the silica bodies were attached to the circular craters, which were spread relatively uniformly over the EFB strands, as in a study by Isroi et al. [69]. This was also similar to the SEM micrograph shown in the study by Nurul Hazirah et al. [70]. The silica present in the cell wall acts as a barrier in the enzymatic digestibility and fermentation process [48]. However, after the pretreatment process was performed, the silica bodies were mostly removed from the EFBs' structure (Figure 2c,d). The remaining holes had homogenous dimensions of around 10 μm in diameter on the EFBs' outer surface [55]. The EFBs' structure became cleaner and smother where almost all the impurities on the EFBs surface were removed, as in the study by Norul Izani et al. [65]. The silica bodies also can be dislodged by an extensive treatment of the EFBs, such as hammering, washing, and crushing [69].

3.1.3. Fourier Transform Infrared Spectroscopy (FTIR) Analysis of EFBs

The structure of EFBs before and after the pretreatment was analyzed using the FTIR spectroscopy method. Based on Figure 3, the pattern of the graph and the existence peaks were different before and after the pretreatment. The basic elements and functional groups present in EFBs were obtained by FTIR analysis [70]. From the FTIR analysis performed by Eliza et al. [71], the presence of a new group was proven after the EFB pretreatment.

(**a**)

(**b**)

(**c**)

(**d**)

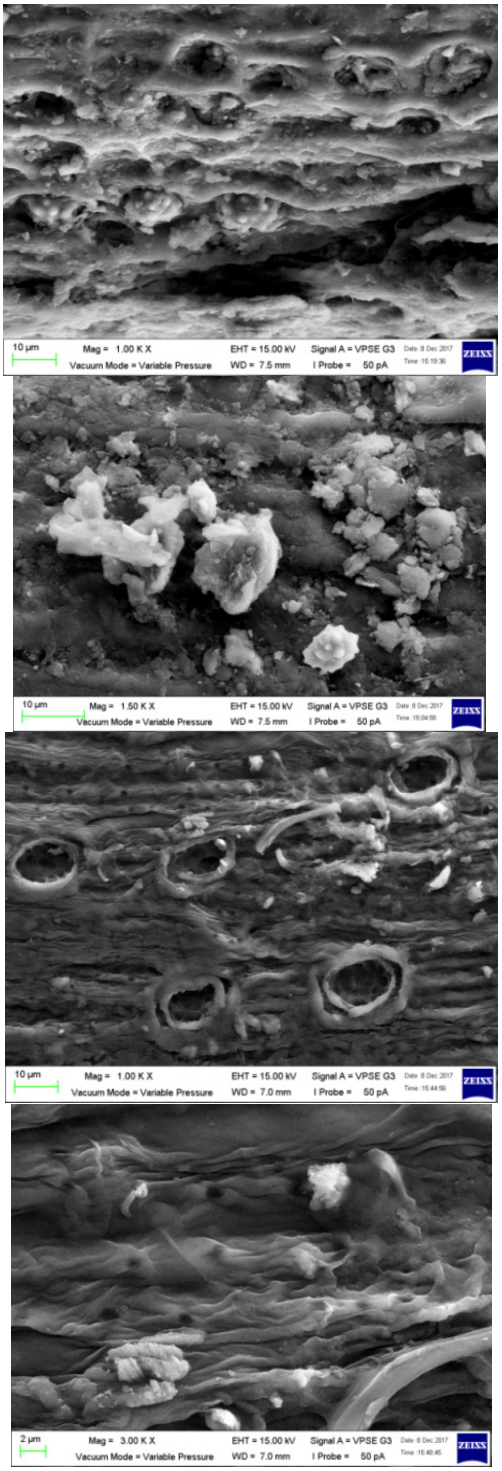

Figure 2. The EFB samples' structure from SEM analysis before and after the pretreatment process: (**a**) untreated EFBs at 1.0K× magnification; (**b**) untreated EFBs at 1.50K× magnification); (**c**) treated EFBs at 1.0K× magnification and (**d**) treated EFBs at 3.0K× magnification).

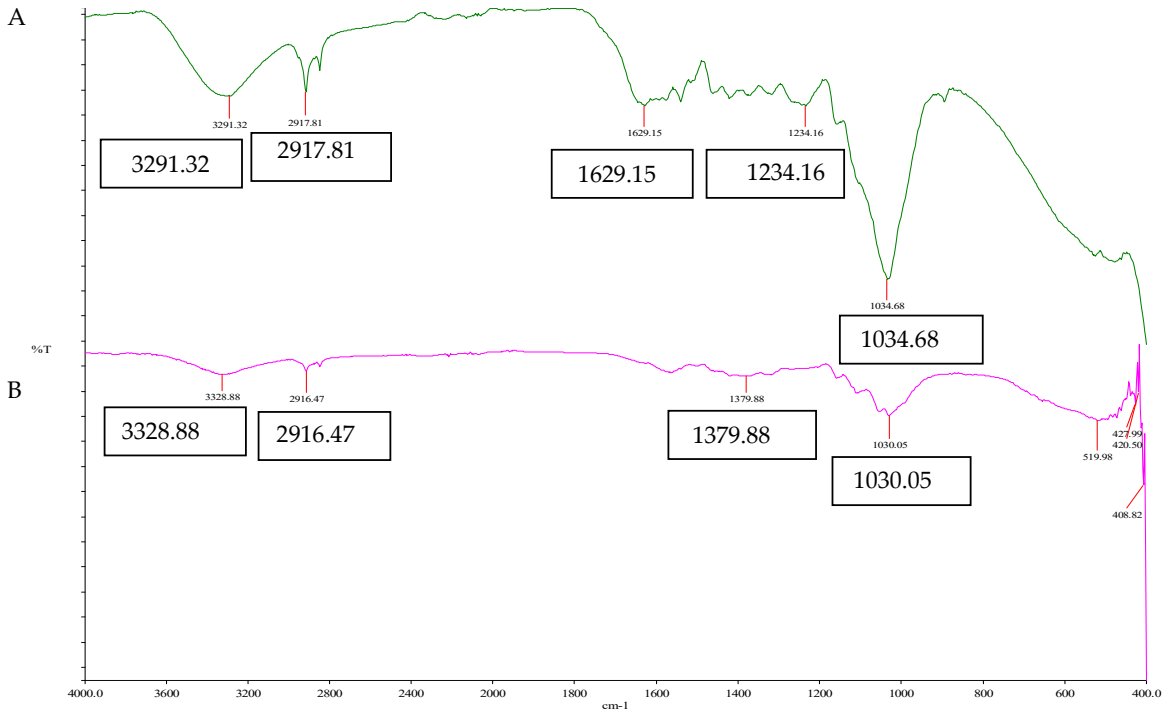

Figure 3. The EFB samples' FTIR analysis before and after the pretreatment process: (**A**) untreated EFBs, (**B**) treated EFBs.

From the figure, absorption bands at 1629.15, 1234.16, and 1034.68 cm^{-1} are shown to have disappeared or diminished, while other bands at 1379.88 and 1030.05 cm^{-1} notably decreased. According to Baharuddin et al. [55], the disappearance of the absorption occurs due to the decomposition of the hemicellulose component in the EFBs. The reduction in the peak intensity shows an indication that the functional group was disturbed or altered [72]. The difference in spectra also can be seen between the untreated and treated EFBs. Changes in the absorption bands were also visible, as some of the peaks became broader after the pretreatment process. The absorption of bands at 3291.32 and 2917.81 cm^{-1} of untreated EFBs was sharp but became broader in the treated EFBs at absorption bands of 3328.88 and 2916.47 cm^{-1}. These changes suggested a decrease in the silica component after the pretreatment process [55].

From the FTIR result, the EFB spectrum shows a strong similarity in the first peak before and after the pretreatment process at absorption bands of 3291.32 and 3328.88 cm^{-1} indicating the presence of hydroxyl (OH) groups in the aromatic and aliphatic compounds [64]. The absorption peak at 2917.81–2916.47 cm^{-1} (second peak) was also identified, which is attributed to the stretchiness of the C-H bonds of the methyl group. The peaks at 1629.15 and 1379.88 cm^{-1} represent the stretching of (C=C) and (C-C), respectively, in aromatics derived from EFBs. Peaks at 1234.16 cm^{-1} could be assigned to the (C-O) bonds of alcohol groups in ethers. The peaks at 1034.68 and 1030.05 cm^{-1} are attributed to glycosidic bonds, indicating the characteristic of cellulose [70]. In another study [55], the most intensive broad absorption band appeared in the carbohydrate region at 1034.68 cm^{-1}, assigned to the vibrations of $C_6H_20_6H$ and C_3HO_3H of the cellulose and pyranosyl ring.

3.2. Enzymatic Saccharification of Pretreated EFBs

The glucose production was determined using high-performance liquid chromatography (HPLC) every 24 h, up to 72 h of the saccharification process. The enzymatic saccharification was performed using cellulase and β-glucosidase, as reported by Hamzah et al. [73]. The highest initial glucose concentration from the pretreated EFBs was achieved at 72 h with 21.14 ± 1.49 g/L. Meanwhile, the initial glucose concentration at 24 and 48 h were

13.827 ± 2.813 g/L and 20.295 ± 1.308 g/L respectively. During the saccharification process, the cellulose in the EFBs was converted to glucose [39].

The enzymatic saccharification of pretreated EFBs was performed to determine the maximum glucose concentration which can be produced during the saccharification. The maximum glucose production was observed at 72 h of incubation with 21.14 ± 1.49 g/L. A similar result has also been reported by Abu Bakar et al. [74], in which the maximum reducing sugars reported was 6.86 g/L at 72 h. According to Adela et al. [32] the longer the enzymatic saccharification time, the higher the glucose yield obtained from the saccharification process. In another study by Hossain et al. [75] the result showed that the glucose content for the oil palm waste residue continuously increased with the increase in the hydrolysis time. The high concentration of the reducing sugars was not only due to the cellulase activity, which produces glucose, but it also can be attributed to the hemicellulases in the biomass [73]. The characteristics of lignocellulosic biomass feedstocks and their pretreatment method in the research influence the performance of cellulase during the enzymatic saccharification process [76].

3.3. Microbial Consortium of S. cerevisiae and T. harzianum

3.3.1. Morphology of the Microbial Consortium of *S. cerevisiae* and *T. harzianum*

Microbes in a consortium are able to use a broad range of carbon sources. Therefore, the microbes can perform complex functions that are impossible for a single type of microorganism [77]. A microbial consortium of *S. cerevisiae* and *T. harzianum* was used as the fermenting microorganisms during the fermentation process. Each microbial strain was cultured independently and then co-cultured together in the same plate, as in Figure 4a–c. The morphologies of yeast and fungi strains were also studied based on their microscopic morphology, as in Figure 4d–f. The morphology of the microbes cultured was observed under the microscope before being used as inoculums in the fermentation process to ensure healthy and pure cells were used in this research. This is to avoid unrelated microbes being inoculated and isolated into the fermentation broth during the fermentation.

(**a**)

(**b**)

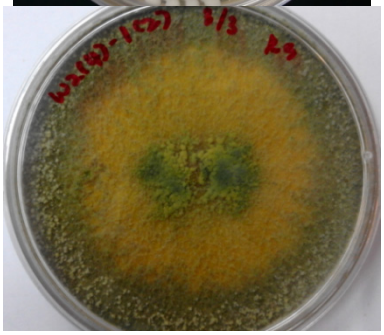

Figure 4. *Cont.*

(**c**)

(**d**)

(**e**)

(**f**)

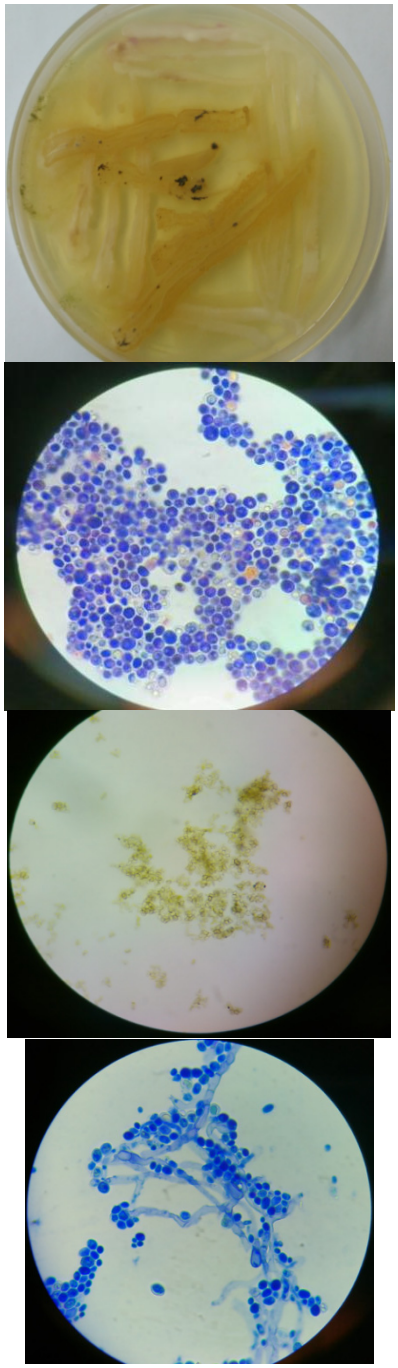

Figure 4. Pure culture: (**a**) yeast *S. cerevisiae*; (**b**) fungi strain *T. harzianum;* (**c**) microbial consortium of *S. cerevisiae* and *T. harzianum*. Morphology: (**d**) *S. cerevisiae*; (**e**) *T. harzianum;* (**f**) microbial consortium of *S. cerevisiae* and *T. harzianum*.

Figure 4a,c shows the pure culture of *S. cerevisiae* and the cells' microscopic view on day 3 of culturing. The *S. cerevisiae* cells that were observed under the microscope were generally round, globular, and ellipsoid in shape, having a diameter of approximately 2–8 µm in length, and most of the cells were attached and elongated to each other. Kusfanto et al.'s [78] result showed that the *S. cerevisiae* cells were usually round or oval-shaped with various sizes. Cells reproduce through a process called budding, and a typical yeast cell is around 5–10 µm in diameter [79]. From the figure, some of the cells observed formed budding. Budding formation indicates the cell division process, in which the "mother" cells

produce an ellipsoidal daughter cell. *S. cerevisiae* is one of the most common microbes used in producing bioethanol while *T. harzianum* is reported to produce the cellulase enzyme, which helps in the fermentation process [80].

The microscopic morphology of *Trichoderma* isolates was observed with 100X magnification under the light microscope in Figure 4d. The shapes, colors, and sizes of conidia were also observed. The conidia cells have ovoidal shapes and were mostly single-celled. The colors of the conidia of *Trichoderma* were found to be green. Conidiophores were many-branched, hyaline, and bearing a single or group of phialides. Phialides were usually flask-shaped, had a slightly narrowed base, and were also swollen in the middle with a pointed tip. Conidia were single-celled, green, and ovoid with rough or smooth walls generally borne in small terminal clusters. A few conidia cells were found to be slightly ovoidal shaped [81]. The *T. harzianum* colonies, which were grown in the PDA plates, should be white at the early stage but turn to a dark green color after 7 days of culturing [82]. The production of *T. harzianum* green conidia on the PDA plate was denser in the center [83]. Different intensities of green colors of mature conidia which were light green, dark green, yellowish-green, and grayish-green can be observed on the PDA plate, as in Figure 4b. PDA was the best medium in terms of biomass yield and growth spore production [84].

The morphological characteristics of the microbial consortium of *S. cerevisiae* and *T. harzianum* were also observed under the light microscope at 100× (Figure 4f). From the figure, both the fungal hyphae of the *T. harzianum* and yeast *S. cerevisiae* cells were observed. In the co-culture of *S. cerevisiae* and *T. reesei* on PDA and LM mixed with cassava, the fungal hyphae also grew with yeast cells when observed under a compound microscope at 100X magnification [85]. From the figure, it is shown that the co-culture has conidiophores with paired primary branches where their phialides were flask or cylindrical in shape. In a study conducted by Prajankate and Sriwasak [85], the white colonies of the *S. cerevisiae* were covered by the green *T. reesei* mycelium after culturing on the PDA plates at 37 °C for 5 days, as in Figure 4c.

In recent years, research has been more focused on bioprocesses using the *S. cerevisiae* as a co-culture with *Trichoderma* spp., due to better fermentation attributes in the conversion of a complex form of carbohydrates into glucose and then the conversion of glucose to ethanol and CO_2 [86]. A microbial consortium is considered a prospective bioprocess if each microorganism metabolizing its substrate is not disturbed by the presence of another microorganism [19]. According to Kumar et al. [87], *S. cerevisiae* and *Actinomyces* co-culture fermentation resulted in higher bioethanol production from apple pomace with 49.64 g/L, while employing a culture of *S. cerevisiae* alone produced only 37.6 g/L ethanol. Swain et al. [33] mentioned that the ability of bioethanol production from un-saccharified sweet potato flour using *S. cerevisiae* and *Trichoderma* spp. co-culture was 65% higher than employing a single culture of *S. cerevisiae*.

3.3.2. Growth Curve of *S. cerevisiae*, *T. harzianum*, and the Co-Culture of *S. cerevisiae* and *T. harzianum*

Figure 5 shows the growth curve of S. cerevisiae, *T. harzianum*, and the co-culture of *S. cerevisiae* and *T. harzianum* by measuring the optical densities of the suspension cultures every 3 h for 48 h at a wavelength of 600 nm [34]. OD is generally used to determine the inhibitory activity of antifungal compounds [88]. Microbes should be harvested at the exponential phase before being inoculated into the fermentation medium for bioethanol production. It is difficult to obtain a higher yield of bioethanol due to the slow growth of microbes from the depletion of nutrients [20]. Hence, the growth of the yeast and fungi was studied.

The growth curve of yeast *S. cerevisiae* showed a short lag phase while the log phase had the sharpest slope and lasted nine hours. From the figure, the logarithmic phase of the yeast *S. cerevisiae* was between the 3rd to 12th hours after the onset of the inoculation. In the first three hours, there was a slight increase in the growth of the yeast culture. Subsequently, the growth increased gradually from the 3rd h, (0.395 ± 0.013) to the 12th h (1.029 ± 0.005).

From the 12th to the 18th h, a slow increase in the growth of the yeast was observed with absorbances of 1.029 ± 0.005, 1.035 ± 0.006, and 1.037 ± 0.007, respectively. The growth curve reached a maximum point at the 21st h, at which the absorbance was recorded at 1.129 ± 0.003. After the maximum growth was achieved, the absorbance of yeast culture was in a stationary pattern until the 48th h (1.089 ± 0.009). There were no major observable changes shown in the growth curve of yeast *S. cerevisiae* from hours 21 to 48.

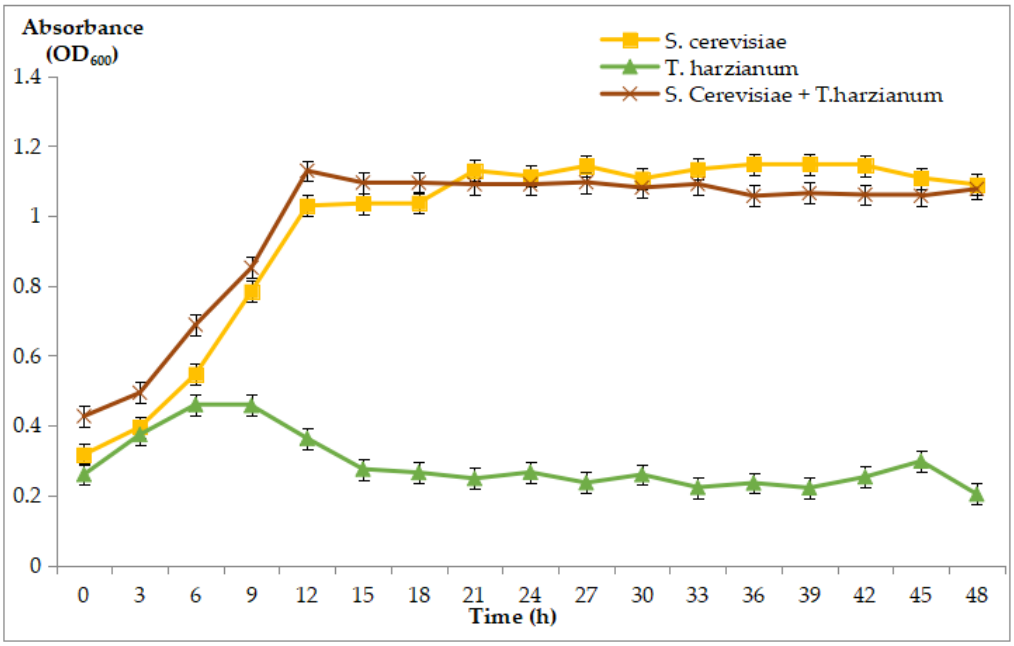

Figure 5. Growth curve of *S. cerevisiae*, *T. harzianum*, and a microbial consortium of *S. cerevisiae* and *T. harzianum*.

The growth curve of fungi *T. harzianum* demonstrated an increasing trend from the 3rd h until the 6th h. These can be seen in the absorbance reading, increasing from 0.374 ± 0.009 to 0.460 ± 0.007. However, the absorbance reading started to decrease from the 9th (0.457 ± 0.004) to the 15th (0.275 ± 0.003) hours. Then, the growth pattern of the fungi was in a stationary state until the 48th h (0.204 ± 0.002). The absorbance reading of the fungi *T. harzianum* showed a much lower reading compared to the yeast *S. cerevisiae* and the co-culture of *S. cerevisiae* and T. harzianum. Absorbance reading or using OD for the filamentous fungi was not so accurate because the hyphae that were growing were not distributed evenly in the microplate well. Thus, there are uncertainties in the estimation of the fungal growth in the medium. Moreover, a higher OD reading might occur due to the sporulation occurring on the surface of the wells, which gives an overestimation of growth. OD reading is, therefore, more suitable for growth vs. no growth studies or for the initial detection of mold growth [88].

For the growth curve of the co-culture *S. cerevisiae* and *T. harzianum*, the growth was increased from the 3rd h to the 12th h and started to enter the stationary phase from the 15th to the 48th h. There was a gradual increase in the growth of the co-culture for the first three observations (3rd, 6th, and 9th hour) with an absorbance reading of 0.494 ± 0.048, 0.688 ± 0.038, and 0.851 ± 0.002 respectively. At the 12th h, the absorbance reading was the highest growth of the co-culture with an absorbance reading of 1.129 ± 0.051. From the 15th (1.095 ± 0.005) to 48th (1.077 ± 0.015) hours, the yeast growth was slowed down, which eventually became a stationary phase.

The growth curve of yeast *S. cerevisiae* and the co-culture *S. cerevisiae* and *T. harzianum* was similar compared to the growth curve of fungi *T. harzianum*. The yeast and co-culture cells had a predictable pattern of growth which can be divided into lag, log, deceleration, and stationary phases [89]. In the lag phase, no growth occurs as the cell culture is adapting

to its environment. Microorganisms are biochemically active in the lag phase but they are not dividing [44]. During the log phase, the cells are growing and dividing rapidly [89]. The cells then reach a stationary phase, where no growth occurs. This is because the cell numbers reach a maximum point at which the cell numbers stop increasing [44]. For the inoculation into the EFBs during the fermentation process, the microorganism cells were harvested at the early exponential phase, which was after 12 h of incubation.

3.4. Selection of Microorganisms and Enzyme Combinations

The selection of microbes (*S. cerevisiae* and *T. harzianum*) and enzymes (cellulase and β-glucosidase) was carried out by comparing the bioethanol concentration after the fermentation process, as in Figure 6 From the figure, the combination of *S. cerevisiae* and *T. harzianum* and enzymes (Cellulase and β-glucosidase) had better results in the conversion of the EFBs into bioethanol production.

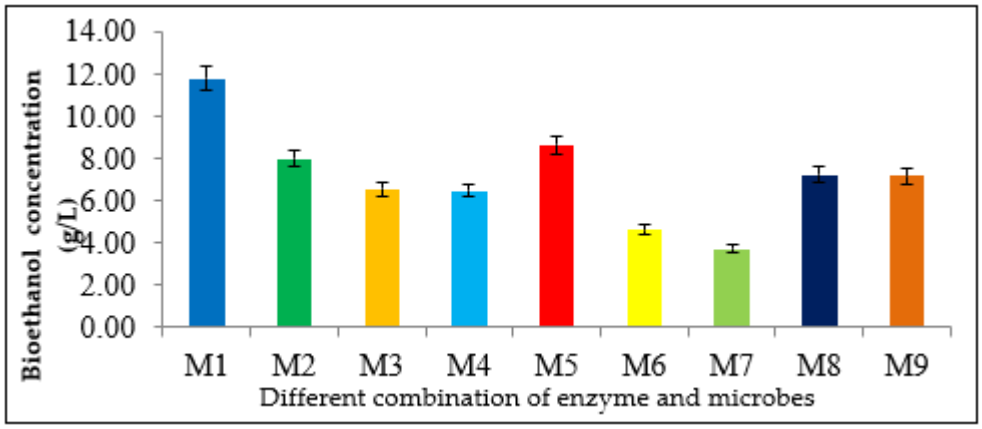

Figure 6. Comparison of Bioethanol concentration from the selection experiment.

From the results obtained, it can be seen that there is a significant difference in the bioethanol production of each run using the empty fruit bunches. According to the figure, M1 had the highest bioethanol concentration with a mean of 11.76 ± 0.79 g/L. Based on previous studies, a combination of the enzymes cellulase and β-glucosidase was successfully employed as the main enzymes for bioethanol production, according to the studies reported by Cui et al. [24], Jung et al. [90], Raman and Gnansounou [91], and Sudiyani et al. [40]. Enzyme cellulase possesses a different catalytic potential for cellulose breakdown and saccharification into fermentable sugar glucose [92]. The Addition of the β-glucosidase enzyme will help in attaining good cellulose hydrolysis performance by breaking down the cellobiose and cellotriose into glucose monomers [93]. Shokrkar et al. [94] described that β-glucosidase promoted the enzymatic hydrolysis process of algal cellulose by increasing the production rate of glucose and decreasing the cellobiose inhibition. A previous study by Poornejad et al. [95] reported that the glucose yield of untreated straw was increased significantly from 25.7% to over 75% for the treated straw during the saccharification process using cellulase and β-glucosidase enzymes. The results of these studies proved that the combinations of cellulase and β-glucosidase were better in enhancing bioethanol production than the single enzyme treatment when combined together with the fermenting microorganisms.

Moreover, a combination of co-cultured *S. cerevisiae* and *T. harzianum* was found to be better as the fermentative microorganisms than using the *S. cerevisiae* and *T. harzianum* independently in the SSF process. The combination of *S. cerevisiae* and *T. harzianum* was found to be the best compatible mixed culture for maximum bioethanol production using EFBs in the solid-state bioconversion process compared to other combinations [26,96]. In addition, *T. harzianum* is a prolific enzyme producer that aids in facilitating the saccharification of EFBs, as it is regarded as a potential cellulase enzyme producer [97,98]. The

co-culture of ethanol-fermenting and amylolytic microorganisms has also shown great potential in making a cost-competitive SSF process for bioethanol production [99]. A study by Verma et al. [100] shows that the ethanol production by a co-culture of *S. diastaticus* and *S. cerevisiae* 21 (24.8 g/L) was higher than the monoculture of *S. diastaticus* (16.8 g/L) using raw, unhydrolyzed starch. According to Dey et al. [101], the co-cultivation of Baker's yeast *S. cerevisiae* and *P. stipitis* NCIM 3499 also resulted in a higher ethanol concentration of 42.34 g/L with 0.53 g/g yield from 18% (*w*/*w*) solid loading of pulp and paper sludge waste. Similarly, Izmirlioglu and Demirci [30], observed a maximum amount of bioethanol production at 35.9 g/L when *A. niger* and *S. cerevisiae* were co-cultured for the SSF of industrial waste potato mash. Liu et al. [102] obtained a 5.825 g/L ethanol yield (40.84% of theoretical yield) by using mixed cultures of *Trichoderma*, *S. cerevisiae*, and *Penicillium* for the bioethanol production of alkali-pretreated wheat bran.

3.5. SSF Optimization for Bioethanol Production

In simultaneous saccharification and fermentation, the enzymes and microbes will be simultaneously converted into ethanol [52]. Therefore, the optimization of the SSF process is important in order to achieve maximum bioethanol production from EFBs at a minimal cost [103]. Four parameters, including fermentation time, temperature, pH, and inoculum concentration, which have a significant influence on fermentation, were optimized using CCD-based RSM. The experimental design and response for the optimization of the SSF process of pretreated EFBs were as in Table S1. The interactive effect of the independent variables was studied in order to obtain optimum conditions for bioethanol production. A good correlation between the experimental and predicted bioethanol concentration from different parameters was observed. This indicates the high accuracy of the response surface model constructed in this experiment.

Further data analysis of the results obtained was performed using the RSM software to determine the suitable model that best fits the experimental data. A quadratic model was suggested as the model because the p-value was statistically significant with a *p*-value of <0.0001 (Table S2). The R2 value at 0.9633 was close to 1, hence indicating the high accuracy of this model and signifying a better correlation between the observed and predicted values [87]. The adjusted R2 of 0.9266 was in agreement with the predicted R2 of 0.7774. Adequate precision compares the average prediction error to the range of the predicted values at the design points [9]. Moreover, the lack of fit value of 2.95 implies that the lack of fit model was not significant relative to the pure error. There is a 15.41% (*p*-value of 0.1541) chance that a lack of fit value this large could occur due to noise. The experimental responses fit with the model when the lack of fit value obtained was not significant in the experiment and could be used to predict the optimum conditions accurately [18].

From the analysis of variance (ANOVA) (Table S3), the Model F-value of 26.25 implies that the model is significant. The ANOVA focused on the relationship between the independent and dependent variables based on the results and data obtained [66]. Based on the ANOVA, eight model terms, fermentation time (A), temperature (B), inoculum concentration (D), the interaction of fermentation time and inoculum concentration (AD), the interaction of temperature and pH (BC)), fermentation time (A2), temperature (B2) and inoculum concentration (D2), were found to be statistically significant with a p-value of less than 0.05 (<0.05), which affects the fermentation. The values of coefficient of variation (C.V. % = 8.37), standard deviation (SD = 0.59), and predicted residual sum of squares (PRESS = 29.69) were relatively low, which explained that the model had good precision and the experiments were reliable.

Final Equation in Terms of Coded Factors:

$$\begin{aligned}&\text{Bioethanol concentration (g/L)}\\&= 8.48 + 1.79\,(A) - 0.34\,(B) + 0.09\,(C) + 0.31\,(D) - 0.31\,(AB) - 0.074\,(AC) - 0.46\,(AD)\\&\quad 0.38\,(BC) - 0.043\,(BD) + 0.041\,(CD) - 1.14\,(A2) - 0.42\,(B2) - 0.021\,(C2) - O.26\,(D2)\end{aligned} \quad (4)$$

Note: A denotes the fermentation time (h), B is the temperature (°C), C is pH, and D is the inoculum concentration (% (*v*/*v*)).

Figure 7a–f shows the 3D response surface plots analysis of the CCD model for the optimized conditions during fermentation. Each figure represents the effect of two different variables on bioethanol production while the other conditions were kept constant at their optimum points [104]. The surface plots show the significant influences of each parameter on bioethanol production in this study. It is also used to investigate the interaction among the parameters and to determine the optimum concentration of each variable for maximum bioethanol production from EFBs [103]. The significant loss of EFBs during pretreatment, incomplete hydrolysis, inefficient fermentation conditions, and type has been identified as a major limitation that leads to poor yield in bioethanol production [105]. Hence, an optimization process was performed to improve the fermentation parameters which influence the bioethanol production efficiency of EFBs. In this study, the effects of fermentation time, temperature, pH, and inoculum concentration on bioethanol production were studied. From the 3D response surface plot analysis, the optimum predicted conditions for bioethanol production from EFBs were: 72 h fermentation time, temperature 30 °C, pH 4.8, and 10% (*v*/*v*) inoculum concentration. Under the above conditions, the maximum experimental bioethanol production was found to be 9.95 g/L, while the predicted response was 9.46 g/L.

(**a**)

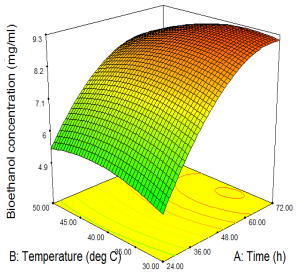

(**b**)

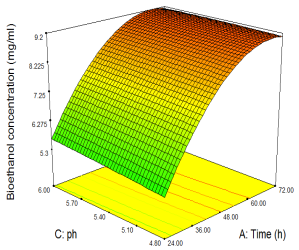

(**c**)

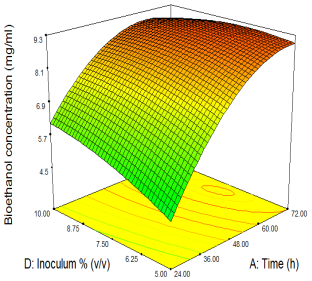

Figure 7. *Cont.*

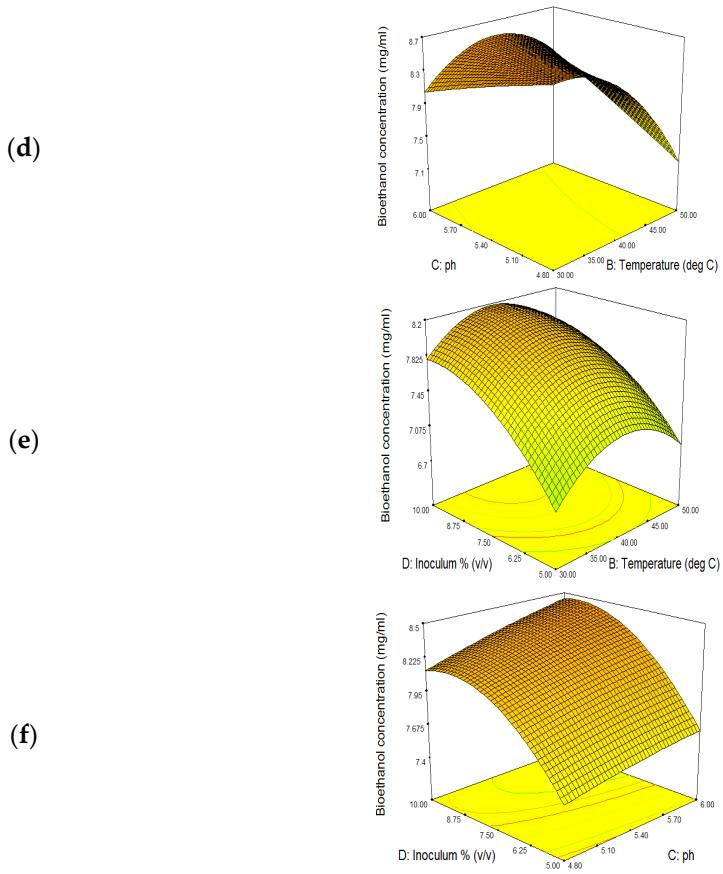

Figure 7. The three-dimensional (3D) surface plot of interaction in the fermentation process based on optimized conditions: (**a**) temperature and time; (**b**) pH and time; (**c**) inoculum concentration and time; (**d**) pH and temperature; (**e**) inoculum concentration and temperature; and (**f**) inoculum concentration and pH. (Note: the area of optimum conditions for fermentation is represented by the darker region).

3.5.1. Effect of Fermentation Time

From the studies, the highest bioethanol concentration obtained was 9.95 ± 0.41 g/L at 72 h while the lowest was 3.35 ± 0.56 g/L at 24 h. The highest bioethanol concentration was produced at a longer fermentation time of 72 h. Bioethanol production gradually increased from 24 to 72 h since the fermentable sugars were sufficient for the growth of microorganisms in order to digest the sugars into bioethanol. It can be seen that the bioethanol concentration tends to increase with the time of fermentation until all the fermentable sugars in the medium are completely utilized by the fermenting microbes. The bioethanol production was found to decrease slightly after 72 h [39].

In this current study, it can be seen that a fermentation time of 60 to 72 h shows a good correlation to the bioethanol production of EFBs. In [93], the bioethanol concentration improved with the increase in fermentation time using the co-culture of *T. harzianum* and *S. cerevisiae* of EFBs. The optimum fermentation time, 72 h was found as a suitable period to obtain higher bioethanol production. Similar results have also been reported by Syadiah et al. [106], in which the maximum ethanol production from sweet sorghum bagasse using a co-culture of *S. cerevisiae* and *Trichoderma reesei* was obtained at 72 h of fermentation with 6.60 g/L. Jambo et al. [107] revealed that the optimum fermentation time for bioethanol production from Eucheuma cottonii based on CCD was also 72 h.

3.5.2. Effect of Temperature

The highest bioethanol (9.95 ± 0.41 g/L) concentration was obtained at 30 °C. High temperature has been shown to lower bioethanol production [108]. Temperature has a

major effect on bioethanol fermentation. The optimum temperature of the enzymes and yeast *S. cerevisiae* growth was 50 °C and 28 °C, respectively [44]. In this study, a new combination of enzymes (Cellulase and β-glucosidase) and microorganisms (*S. cerevisiae* and *T. harzianum*) were employed in the SSF fermentation process. Every enzyme and microorganism has its own optimum temperature for every process. Therefore, it is important to strike a balance between the optimal temperature for the enzymes and microorganisms used in the fermentation [109]. Thus, the optimization process for the parameter of temperature (30 °C to 50 °C) was carried out in the SSF fermentation.

In this study, the optimum temperature for the highest bioethanol production using co-cultures in EFBs was observed to be 30 °C. The cellulolytic enzyme activity shows a maximum at 30 °C in co-culture conditions in the present study, which might due to one of the enzymes; cellulase is derived from the microorganism *Trichoderma reesei*. Thus, the cellulolytic activity, which works best at 30 °C, influenced the glucose production from cellulase. This result is in accordance with the study of Ahmad et al. [110], in which the optimum temperature for maximum ethanol production was at a temperature of 30 °C. The ethanol yield was decreased significantly when temperature values were higher or lower than 30 °C. However, Verma et al. [100] suggested that a slight difference in temperature between 30 °C and 40 °C will not affect the ethanol fermentation of starch using a co-culture of *S. cerevisiae* and *S. diastaticus*. Research by Kassim et al. [111] reported that the lowest ethanol production rate was at 40 °C compared to other temperatures at 30 °C and 35 °C. This is because fermentation at higher temperatures can inhibit ethanol production. Moreover, a decrease in the viable cell number at temperatures above 30 °C would lower the bioethanol concentration and fermentation efficiency [33]. According to Park et al. [20], the optimal temperature for ethanol production using a fed-batch from the alkali-pretreated EFBs was 30 °C. Sahu et al. [112] attained the highest bioethanol production with 29.5 g/L at a 30 °C temperature for the fermentation process of glucose for rose petals.

3.5.3. Effect of pH

From the results, the highest bioethanol concentration of 9.95 ± 0.41 g/L was obtained at pH 4.8. In order to determine the effect of pH on the fermentation by the co-culture on bioethanol production, the citrate buffer pH was adjusted in the range of 4.8 to 6.0. In the present study, it was found that pH did not significantly affect the optimization of the fermentation, based on the ANOVA analysis. This occurred because the range of pH chosen for the optimization process was not wide enough to be used in the fermentation process. From the results, both the high (6.0) and low (4.8) pH values showed little difference in bioethanol production.

From the CCD optimization design, it was indicated that the optimum pH value for the fermentation process was 4.8. This shows that the co-culture preferred a slightly acidic condition to grow. Even though acids were required for the production of bioethanol, a highly acidic condition was not suitable for cell growth [113]. In Alam et al. [114], pH 5.5 was found as the optimum pH that led to a maximum bioethanol production of 7.4 g/L using co-cultured *S. cerevisiae* and *A. niger* for EFB fermentation. Meanwhile, Anu et al. [115] exhibited the best attribute for bioethanol production with 18.07 g/L for the enzymatic hydrolysate (20%) of pretreated rice straw at pH 6, 30 °C after 72 h. Meanwhile, the study by Chohan et al. [116] observed an increase in the ethanol yield from 0.14 g/g to 0.29 g/g after the pH was increased from 4.00 to 6.30. However, further increases in pH beyond 6.30 reduced the process yield. Hence, increasing the pH value significantly affected the production of ethanol and the rate of glucose consumption during the fermentation process.

3.5.4. Effect of Inoculum Concentration

According to the results, the highest bioethanol (9.95 ± 0.41 g/L) concentration was produced at 10% (*v*/*v*) inoculum concentration, respectively. These results were in line with the results obtained by Swain et al. [30] for the production of ethanol using sweet potato, in which the optimal inoculum size was 10%. Ansar et al. [117] described that the higher

the percentage of inoculum used during fermentation, the higher the amount of ethanol produced. An increase in the inoculum concentration should increase the concentration of bioethanol. Different inoculum concentrations can be used to determine whether the ethanol yield and productivity were influenced [109]. In this study using the RSM approach, it was found that a high inoculum concentration increased the bioethanol yield.

The inoculum concentration used is one of the most critical factors which influences the industrial fermentation, lag phase duration, biomass yield, specific growth rate, and final product yield [118]. Kabbashi et al. [31] employed a 4% (v/v) inoculum size in the direct solid-state bioconversion of palm oil EFBs for bioethanol production with a maximum ethanol yield of 14.1% (v/v). The research by Neelakandan et al. [119] showed that the optimum inoculum concentration for cashew apple juice for bioethanol production was 8% (v/v) with a maximum bioethanol yield of 7.62% (v/v).

3.6. Bioethanol Production Using Optimized Conditions of Fermentation

The experimental analysis was performed to determine the optimized conditions for the fermentation process. Based on the optimization analysis of the experimental data, the suggested optimum levels of all the variables from the quadratic model of CCD in this study were 72 h of fermentation time, a temperature of 30 °C, pH 4.8, and an inoculum concentration of 6.79% (v/v). From these optimized conditions, the bioethanol concentration can reach up to 9.72 g/L with the desirability of 0.977.

A validation experiment was carried out to evaluate the conditions predicted by the CCD. The fermentation process was conducted under optimized conditions with 72 h of fermentation time, a temperature of 30 °C, pH 4.8, and an inoculum concentration of 6.79% (v/v). The bioethanol concentration after the fermentation process was 9.65 g/L, which was in close agreement with the predicted value of 9.72 g/L. The difference between the predicted and experimental value was only 1.07%. Therefore, it can be concluded that the response surface from this study is reliable to be used to predict bioethanol production from the fermentation process.

4. Conclusions

Empty fruit bunches were treated with sequential acid-alkali pretreatment before being further used as the main feedstock in this study. A change in the physical characteristics and morphology of the EFBs before and after the pretreatment was confirmed by SEM and FTIR analysis. From the SEM analysis, the formation of pores and removal of silica was shown in the treated EFBs' structure. The FTIR spectra of EFBs showed a different graph pattern and peak between the raw and treated EFBs. The combination of enzymes and microorganisms in producing bioethanol was screened to determine the optimum concentration of this combination for the fermentation process of EFBs. It was found that enzyme combinations of cellulase and β-glucosidase with the microorganism combination of *S. cerevisiae* and *T. harzianum* had better results in the conversion of the EFBs into bioethanol production. From the GCMS analysis, this combination has the highest bioethanol concentration with 11.76 ± 0.79 g/L. The simultaneous saccharification and fermentation (SSF) optimization process was performed on pretreated EFBs by employing the central composite design of Response Surface Methodology. The effects of fermentation time, temperature, pH, and inoculum concentration on the fermentation were then analyzed. During fermentation, the highest bioethanol concentration was obtained at 72 h, 30 °C, pH 4.8, and an inoculum concentration of 10% (v/v). Based on the CCD analysis, the SSF of pretreated EFBs was repeated using the optimized conditions. From the results, the experimental data obtained were in close agreement with the RSM model prediction. Thus, it can be deduced that the RSM optimization of EFBs using SSF employed in this study is a promising tool for the better optimization of the fermentation process of bioethanol production in the future. Moreover, a new combination of enzymes and microbes was employed in the fermentation process. This combination has never been employed in other studies related to bioethanol production from EFBs using simultaneous saccharification and fermentation. Hence, this

study can be a pioneer for the development of bioethanol production, as the results obtained were satisfactory with regard to bioethanol yield. Moreover, the employment of a central composite design from the RSM method for the optimization of the SSF process in this study showed a promising potential for the production of bioethanol using lignocellulosic biomass waste in the future. Thus, this study may contribute to future research for second-generation bioethanol using lignocellulosic biomass waste in Malaysia. In addition, the potential of EFBs as the main feedstock may contribute to the economic development of Malaysia by producing bioethanol, which is commercially valuable.

Supplementary Materials: The following are available online at https://www.mdpi.com/article/10.3390/fermentation8070295/s1, Table S1: Experimental design and responses for the simultaneous saccharification and fermentation process of pretreated EFBs for bioethanol production. Table S2: Model summary statistics of central composite design for the optimization of simultaneous saccharification and fermentation. Table S3: Analysis of variance table (ANOVA).

Author Contributions: E.D.; conceptualization, investigation, formal analysis, data curation, methodology, writing—original draft. R.A.; supervision, conceptualization, overall guidance, writing—review and editing, validation, revision of the paper. H.M.; writing—review and editing. M.K.S.; writing—review and editing. J.A.G.; writing—review and editing. P.R.; writing—review and editing. All authors have read and agreed to the published version of the manuscript.

Funding: This research received no external funding.

Institutional Review Board Statement: This study did not require any ethical approval.

Informed Consent Statement: Not applicable.

Data Availability Statement: Not applicable.

Acknowledgments: The authors would like to thank and acknowledge the Ministry of Education Malaysia (KPM) for financial support through the MyMaster Scholarship and Faculty of Science and Natural Resources, UMS.

Conflicts of Interest: The authors declare no conflict of interest.

References

1. Chen, J.; Zhang, B.; Luo, L.; Zhang, F.; Yi, Y.; Shan, Y.; Bianfang, L.; Yuan, Z.; Xin, W.; Xin, L. A review on recycling techniques for bioethanol production from lignocellulosic biomass. *Renew. Sustain. Energy Rev.* **2021**, *149*, 111370. [CrossRef]
2. Hosseinzadeh-bandbafha, H.; Nazemi, F.; Khounani, Z.; Ghanavati, H. Safflower-based biorefinery producing a broad spectrum of biofuels and biochemicals: A life cycle assessment perspective. *Sci. Total Environ.* **2022**, *802*, 149842. [CrossRef]
3. Hanif, M.; Mahlia, T.M.I.; Aditiya, H.B.; Chong, W.T. Techno-economic and environmental assessment of bioethanol production from high starch and root yield Sri Kanji 1 cassava in Malaysia. *Energy Rep.* **2016**, *2*, 246–253. [CrossRef]
4. Thakur, A.K.; Kaviti, A.K.; Mehra, R.; Mer, K.K.S. Progress in performance analysis of ethanol-gasoline blends on SI engine. *Renew. Sustain. Energy Rev.* **2017**, *69*, 324–340. [CrossRef]
5. Masum, B.M.; Masjuki, H.H.; Kalam, M.A.; Fattah, I.M.R.; Palash, S.M.; Abedin, M.J. Effect of ethanol—Gasoline blend on NOx emission in SI engine. *Renew. Sustain. Energy Rev.* **2013**, *24*, 209–222. [CrossRef]
6. Zabed, H.; Sahu, J.N.; Suely, A.; Boyce, A.N.; Faruq, G. Bioethanol production from renewable sources: Current perspectives and technological progress. *Renew. Sustain. Energy Rev.* **2017**, *71*, 475–501. [CrossRef]
7. Ahmad, A.; Buang, A.; Bhat, A.H. Renewable and sustainable bioenergy production from microalgal co-cultivation with palm oil mill effluent (POME): A review. *Renew. Sustain. Energy Rev.* **2016**, *65*, 214–234. [CrossRef]
8. Derman, E.; Abdulla, R.; Marbawi, H.; Sabullah, M.K. Oil palm empty fruit bunches as a promising feedstock for bioethanol production in Malaysia. *Renew. Energy* **2018**, *129*, 285–298. [CrossRef]
9. Khairil Anwar, N.A.K.; Hassan, N.; Mohd Yusof, N.; Idris, A. High-titer bio-succinic acid production from sequential alkalic and metal salt pretreated empty fruit bunch via simultaneous saccharification and fermentation. *Ind. Crop Prod.* **2021**, *166*, 113478. [CrossRef]
10. Anita, S.H.; Fitria; Solihat, N.N.; Sari, F.P.; Risanto, L.; Fatriasari, W.; Risanto, L.; Fatriasari, W.; Hermiati, E. Optimization of Microwave-Assisted Oxalic Acid Pretreatment of Oil Palm Empty Fruit Bunch for Production of Fermentable Sugars. *Waste Biomass Valorization* **2019**, *11*, 2673–2687. [CrossRef]
11. Chang, S.H. An overview of empty fruit bunch from oil palm as feedstock for bio-oil production. *Biomass Bioenergy* **2014**, *62*, 174–181. [CrossRef]

12. Tan, L.; Wang, M.; Li, X.; Li, H.; Zhao, J.; Qu, Y.; Choo, Y.M.; Loh, S.K. Fractionation of oil palm empty fruit bunch by bisulfite pretreatment for the production of bioethanol and high value products. *Bioresour. Technol.* **2016**, *200*, 572–578. [CrossRef] [PubMed]
13. Aditiya, H.B.; Chong, W.T.; Mahlia, T.M.I.; Sebayang, A.H.; Berawi, M.A.; Nur, H. Second generation bioethanol potential from selected Malaysia 's biodiversity biomasses: A review. *Waste Manag.* **2016**, *47*, 46–61. [CrossRef] [PubMed]
14. Piarpuzan, D.; Quintero, J.A.; Cardona, C.A. Empty fruit bunches from oil palm as a potential raw material for fuel ethanol production. *Biomass Bioenergy* **2011**, *35*, 1130–1137. [CrossRef]
15. Aguilar-reynosa, A.; Romaní, A.; Rodríguez-jasso, R.M.; Aguilar, C.N.; Garrote, G.; Ruiz, H.A. Comparison of microwave and conduction-convection heating autohydrolysis pretreatment for bioethanol production. *Bioresour Technol.* **2017**, *243*, 273–283. [CrossRef]
16. Abo-state, M.A.; Ragab, A.M.E.; El-gendy, N.S.; Farahat, L.A. Bioethanol Production from Rice Straw Enzymatically Saccharified by Fungal Isolates, *Trichoderma viride* F94 and *Aspergillus terreus* F98. *Soft* **2014**, *3*, 19–29. [CrossRef]
17. Javed, M.R.; Noman, M.; Shahid, M.; Ahmed, T.; Khurshid, M.; Rashid, M.H.; Ismail, M.; Sadaf, M.; Khan, F. Current situation of biofuel production and its enhancement by CRISPR /Cas9-mediated genome engineering of microbial cells. *Microbiol. Res.* **2019**, *219*, 1–11. [CrossRef]
18. Sharma, S.; Sharma, V.; Kuila, A. Simultaneous Saccharification and Fermentation of Corn Husk by Co-Culture Strategy. *J. Pet. Environ. Biotechnol.* **2019**, *9*, 360. [CrossRef]
19. Dahnum, D.; Octavia, S.; Triwahyuni, E.; Nurdin, M. Comparison of SHF and SSF processes using enzyme and dry yeast for optimization of bioethanol production from empty fruit bunch. *Energy Procedia* **2015**, *68*, 107–116. [CrossRef]
20. Park, E.Y.; Naruse, K.; Kato, T. One-pot bioethanol production from cellulose by co-culture of *Acremonium cellulolyticus* and *Saccharomyces cerevisiae*. *Biotechnol. Biofuels* **2012**, *5*, 64. [CrossRef]
21. Galbe, M.; Zacchi, G. A review of the production of ethanol from softwood. *Appl. Microbiol. Biotechnol.* **2002**, *59*, 618–628. [CrossRef] [PubMed]
22. Bhutto, A.W.; Qureshi, K.; Harijan, K.; Abro, R.; Abbas, T.; Bazmi, A.A. Insight into progress in pre-treatment of lignocellulosic biomass. *Energy* **2017**, *122*, 724–745. [CrossRef]
23. Rastogi, M.; Shrivastava, S. Recent advances in second generation bioethanol production: An insight to pretreatment, saccharification and fermentation processes. *Renew. Sustain. Energy Rev.* **2017**, *80*, 330–340. [CrossRef]
24. Cui, X.; Zhao, X.; Zeng, J.; Loh, S.K.; Choo, Y.M.; Liu, D. Robust enzymatic hydrolysis of Formiline-pretreated oil palm empty fruit bunches (EFB) for efficient conversion of cellulose to sugars and. *Bioresour. Technol.* **2014**, *166*, 584–591. [CrossRef] [PubMed]
25. Kim, S.; Kim, C.H. Bioethanol production using the sequential acid/alkali-pretreated empty palm fruit bunch fiber. *Renew. Energy* **2013**, *54*, 150–155. [CrossRef]
26. Jung, S.; Shetti, N.P.; Reddy, K.R.; Nadagouda, M.N.; Park, Y.; Aminabhavi, T.M.; Kwon, E.E. Synthesis of different biofuels from livestock waste materials and their potential as sustainable feedstocks—A review. *Energy Convers. Manag.* **2021**, *236*, 114038. [CrossRef]
27. Polprasert, S.; Choopakar, O.; Elefsiniotis, P. Bioethanol production from pretreated palm empty fruit bunch (PEFB) using sequential enzymatic hydrolysis and yeast fermentation. *Biomass Bioenergy* **2021**, *149*, 106088. [CrossRef]
28. Ali, I.W.; Aziz, K.K.; Syahadah, A.A.H. Bioethanol Production from Acid Hydrolysates of Date Palm Fronds Using a Co-culture of *Saccharomyces cerevisiae* and *Pichia stipitis*. *Int. J. Enhanc. Res. Sci. Technol. Eng.* **2014**, *3*, 35–44.
29. Mishra, A.; Ghosh, S. Saccharification of kans grass biomass by a novel fractional hydrolysis method followed by co-culture fermentation for bioethanol production. *Renew. Energy* **2020**, *146*, 750–759. [CrossRef]
30. Izmirlioglu, G.; Demirci, A. Simultaneous saccharification and fermentation of ethanol from potato waste by co-cultures of *Aspergillus niger* and *Saccharomyces cerevisiae* in biofilm reactors. *Fuel* **2017**, *202*, 260–270. [CrossRef]
31. Kabbashi, N.A.; Alam, M.Z.; Tompang, M.F. Direct Bioconversion of Oil Palm Empty Fruit Bunches for Bioethanol Production by Solid State Bioconversion. *IIUM Eng. J.* **2007**, *8*, 25–36. [CrossRef]
32. Adela, N.; Nasrin, A.B.; Loh, S.K.; Choo, Y.M. Bioethanol Production by Fermentation of Oil Palm Empty Fruit Bunches Pretreated with Combined Chemicals. *J. Appl. Environ. Biol. Sci.* **2014**, *4*, 234–242.
33. Swain, M.R.; Mishra, J.; Thatoi, H. Bioethanol Production from Sweet Potato (*Ipomoea batatas* L.) Flour using Co-Culture of *Trichoderma* sp. and *Saccharomyces cerevisiae* in Solid-State Fermentation. *Braz. Arch. Biol. Technol.* **2013**, *56*, 171–179. [CrossRef]
34. Bhadwal, A.S.; Le, A.; Le, T.T.; Shrivastava, S.; Bera, T. *Trichoderma koningii* assisted biogenic synthesis of silver nanoparticles and evaluation of their antibacterial activity. *Adv. Nat. Sci. Nanosci. Nanotechnol.* **2013**, *4*, 35005.
35. Bergman, L.W. Growth and Maintenance of Yeast. In *Methods in Molecular Biology, Two Hybrid Systems: Methods and Protocols*; MacDonald, P.N., Ed.; Humana Press Inc.: Totowa, NJ, USA, 2001; Volume 177, pp. 9–39.
36. Rodrigues, B.; Lima-Costa, M.E.; Constantino, A.; Raposo, S.; Felizardo, C.; Gonçalves, D.; Peinado, J.M. Growth kinetics and physiological behavior of co-cultures of *Saccharomyces cerevisiae* and *Kluyveromyces lactis*, fermenting carob sugars extracted with whey. *Enzym. Microb. Technol.* **2016**, *92*, 41–48. [CrossRef] [PubMed]
37. Paschos, T.; Xiros, C.; Christakopoulos, P. Simultaneous saccharification and fermentation by co-cultures of *Fusarium oxysporum* and *Saccharomyces cerevisiae* enhances ethanol production from liquefied wheat straw at high solid content. *Ind. Crop Prod.* **2015**, *76*, 793–802. [CrossRef]

38. Sasikumar, E.; Viruthagiri, T. Optimization of Process Conditions Using Response Surface Methodology (RSM) for Ethanol Production from Pretreated Sugarcane Bagasse: Kinetics and Modeling. *Bioenergy Resour.* **2008**, *1*, 239–247. [CrossRef]
39. Duangwang, S.; Sangwichien, C. Utilization of Oil Palm Empty Fruit Bunch Hydrolysate for Ethanol Production by Baker's Yeast and Loog-Pang. *Energy Procedia* **2015**, *79*, 157–162. [CrossRef]
40. Sudiyani, Y.; Styarini, D.; Triwahyuni, E.S.; Sembiring, K.C.; Aristiawan, Y.; Han, M.H. Utilization of biomass waste empty fruit bunch fiber of palm oil for bioethanol production using pilot—Scale unit. *Energy Procedia* **2013**, *32*, 31–38. [CrossRef]
41. Baharuddin, A.S.; Nor, A.A.R.; Umi, K.M.S.; Mohd, A.H.; Minato, W.; Yoshihito, S. Evaluation of pressed shredded empty fruit bunch (EFB)-palm oil mill effluent (POME) anaerobic sludge based compost using Fourier transform infrared (FTIR) and nuclear magnetic resonance (NMR) analysis. *Afr. J. Biotechnol.* **2011**, *10*, 8082–8089.
42. Sindhu, R.; Kuttiraja, M.; Prabisha, T.P.; Binod, P.; Sukumaran, R.K.; Pandey, A. Development of a combined pretreatment and hydrolysis strategy of rice straw for the production of bioethanol and biopolymer. *Bioresour. Technol.* **2016**, *215*, 110–116. [CrossRef] [PubMed]
43. Hamouda, H.I.; Nassar, H.N.; Madian, H.R.; Amr, S.S.A.; El-Gendy, N.S. Response Surface Optimization of Bioethanol Production from Sugarcane Molasses by *Pichia veronae* Strain HSC-22. *Biotechnol. Res. Int.* **2015**, *10*, 905792. [CrossRef] [PubMed]
44. Mansa, R.F.; Chen, W.F.; Yeo, S.J.; Farm, Y.Y.; Bakar, H.A.; Sipaut, C.S. Chapter 13: Fermentation Study on Macroalgae Eucheuma cottonii for Bioethanol Production via Varying Acid Hydrolysis. In *Advanced Biofuels*; Sarbatly, R.P.H., Ed.; Springer Science and Business Media: New York, NY, USA, 2013; pp. 219–240.
45. Tan, I.S.; Lee, K.T. Enzymatic hydrolysis and fermentation of seaweed solid wastes for bioethanol production: An optimization study. *Energy* **2014**, *78*, 53–62. [CrossRef]
46. Burhani, D.; Putri, A.M.H.; Waluyo, J.; Nofiana, Y.; Sudiyani, Y. The effect of two-stage pretreatment on the physical and chemical characteristic of oil palm empty fruit bunch for bioethanol production. *AIP Conf. Proc.* **2017**, *1904*, 20016.
47. Campioni, T.S.; Soccol, C.R.; Libardi Junior, N.; Rodrigues, C.; Woiciechowski, A.L.; Letti, L.A.J.; Vandenberghe, L.P.D.S. Sequential chemical and enzymatic pretreatment of palm empty fruit bunches for *Candida pelliculosa* bioethanol production. *Biotechnol. Appl. Biochem.* **2019**, *67*, 723–731. [CrossRef]
48. Akhtar, J.; Teo, C.L.; Lai, L.W.; Hassan, N.; Idris, A.; Aziz, R.A. Factors affecting delignification of oil palm empty fruit bunch by microwave-assisted dilute acid/alkali pretreatment. *BioResources* **2015**, *10*, 588–596. [CrossRef]
49. Ebrahimi, M.; Villaflores, O.B.; Ordono, E.E.; Caparanga, A.R. Effects of acidified aqueous glycerol and glycerol carbonate pretreatment of rice husk on the enzymatic digestibility, structural characteristics, and bioethanol production. *Bioresour. Technol.* **2017**, *228*, 264–271. [CrossRef]
50. Abdul, P.M.; Jahim, M.J.; Harun, S.; Markom, M.; Lutpi, N.A.; Hassan, O.; Mohd Nor, M.T. Effects of changes in chemical and structural characteristic of ammonia fibre expansion (AFEX) pretreated oil palm empty fruit bunch fibre on enzymatic saccharification and fermentability for biohydrogen. *Bioresour. Technol.* **2016**, *211*, 200–208. [CrossRef]
51. Taherzadeh, M.J.; Karimi, K. Pretreatment of Lignocellulosic Wastes to Improve Ethanol and Biogas Production: A Review. *Int. J. Mol. Sci.* **2008**, *9*, 1621–1651. [CrossRef]
52. Sari, A.A.; Ariani, N.; Muryanto; Kristiani, A.; Utomo, T.B.; Sudarno. Potential of Oil Palm Empty Fruit Bunches for Bioethanol Production and Application of Chemical Methods in Bioethanol Wastewater Treatment OPEFB for Bioethanol and Its Wastewater Treatment. In Proceedings of the International Conference on Sustainable and Renewable Energy Engineering, Hiroshima, Japan, 10–12 May 2017; pp. 1–4.
53. Triwahyuni, E.; Muryanto; Sudiyani, Y.; Abimanyu, H. The effect of substrate loading on simultaneous saccharification and fermentation process for bioethanol production from oil palm empty fruit bunches. *Energy Procedia* **2015**, *68*, 138–146. [CrossRef]
54. Fatriasari, W.; Ulwan, W.; Aminingsih, T.; Puspita, F.; Suryanegara, L.; Heri, A.; Ghozali, M.; Kholida, L.N.; Hussin, M.H. Optimization of maleic acid pretreatment of oil palm empty fruit bunches (OPEFB) using response surface methodology to produce reducing sugars. *Ind. Crop Prod.* **2021**, *171*, 113971. [CrossRef]
55. Baharuddin, A.S.; Sulaiman, A.; Kim, D.H.; Mokhtar, M.N.; Hassan, M.A.; Wakisaka, M.; Shirai, Y.; Nishida, H. Selective component degradation of oil palm empty fruit bunches (OPEFB) using high-pressure steam. *Biomass Bioenergy* **2013**, *55*, 268–275. [CrossRef]
56. Paramasivan, S.; Sankar, S.; Velavan, R.S.; Krishnakumar, T.; Sithara, R.; Batcha, I.; Muthuvelu, K.S. Assessing the potential of lignocellulosic energy crops as an alternative resource for bioethanol production using ultrasound assisted dilute acid pretreatment. *Mater. Today Proc.* **2021**, *45*, 3279–3285. [CrossRef]
57. Musatto, S.I.; Dragone, G.; Fernandes, M.; Milagres, A.M.F.; Roberto, I.C. The effect of agitation speed, enzyme loading and substrate concentration on enzymatic hydrolysis of cellulose from brewer's spent grain. *Cellulose* **2008**, *15*, 711–721. [CrossRef]
58. Ariffin, H.; Hassan, M.; Umi Kalsom, M.; Abdullah, N.; Shirai, Y.; Ariffin, H. Effect of physical, chemical and thermal pretreatments on the enzymatic hydrolysis of oil palm empty fruit bunch (OPEFB). *J. Trop. Agric. Food Sci.* **2008**, *36*, 1–10.
59. Kim, D.Y.; Kim, Y.; Kim, T.; Oh, K. Two-stage, acetic acid-aqueous ammonia, fractionation of empty fruit bunches for increased lignocellulosic biomass utilization. *Bioresour. Technol.* **2016**, *199*, 121–127. [CrossRef]
60. Alvira, P.; Tomás-Pejó, E.; Ballesteros, M.; Negro, M.J. Pretreatment technologies for an efficient bioethanol production process based on enzymatic hydrolysis: A review. *Bioresour. Technol.* **2010**, *101*, 4851–4861. [CrossRef]
61. Santosh, I.; Ashtavinayak, P.; Amol, D.; Sanjay, P. Enhanced bioethanol production from different sugarcane bagasse cultivars using co-culture of *Saccharomyces cerevisiae* and *Scheffersomyces* (*Pichia*) *stipitis*. *J. Environ. Chem. Eng.* **2017**, *5*, 2861–2868. [CrossRef]

62. Liong, Y.Y.; Halis, R.; Lai, O.M.; Mohamed, R. Conversion Of Lignocellulosic Biomass From Grass To Bioethanol Using Materials Pretreated With Alkali And The White Rot Fungus, *Phanerochaete Chrysosporium*. *BioResources* **2012**, *7*, 5500–5513. [CrossRef]
63. Thanapimmetha, A.; Saisriyoot, M.; Khomlaem, C.; Chisti, Y.; Srinophakun, P. A comparison of methods of ethanol production from sweet sorghum bagasse. *Biochem. Eng. J.* **2019**, *151*, 107352. [CrossRef]
64. Coral Medina, J.D. Woiciechowski, A.; Zandona Filho, A.; Noseda, M.D.; Kaur, B.S.; Soccol, C.R. Lignin preparation from oil palm empty fruit bunches by sequential acid/alkaline treatment—A biorefinery approach. *Bioresour. Technol.* **2015**, *194*, 172–178. [CrossRef]
65. Norul Izani, M.A.; Paridah, M.T.; Anwar, U.M.K.; Mohd Nor, M.Y.; Ng, P.S. Effects of fiber treatment on morphology, tensile and thermogravimetric analysis of oil palm empty fruit bunches fibers. *Compos. B Eng.* **2013**, *45*, 1251–1257. [CrossRef]
66. Chin, S.X.; Chia, H.C.; Zakaria, S.; Fang, Z.; Ahmad, S. Ball milling pretreatment and diluted acid hydrolysis of oil palm empty fruit bunch (EFB) fibres for the production of levulinic acid. *J. Taiwan Inst. Chem. Eng.* **2015**, *52*, 85–92. [CrossRef]
67. Tye, Y.Y.; Leh, C.P.; Wan Abdullah, W.N. Total glucose yield as the single response in optimizing pretreatments for *Elaeis guineensis* fibre enzymatic hydrolysis and its relationship with chemical composition of fibre. *Renew. Energy* **2017**, *114*, 383–393. [CrossRef]
68. Shamsudin, S.; Md Shah, U.K.; Zainudin, H.; Abd-Aziz, S.; Mustapa Kamal, S.M. Shirai, Y.; Hassan, M.A. Effect of steam pretreatment on oil palm empty fruit bunch for the production of sugars. *Biomass Bioenergy* **2012**, *36*, 280–288. [CrossRef]
69. Isroi; Cifriadi, A.; Panji, T.; Wibowo, N.A.; Syamsu, K. Bioplastic production from cellulose of oil palm empty fruit bunch. *IOP Conf. Ser. Earth Environ. Sci.* **2017**, *65*, 12011. [CrossRef]
70. Nurul Hazirah, C.H.; Masturah, M.; Osman, H.; Jamaliah, M.J.; Shuhaida, H. Preliminary Study on Analysis of the Chemical Compositions and Characterization of Empty Fruit Bunch (EFB) in Malaysia. *Adv. Mater. Res.* **2014**, *970*, 204–208. [CrossRef]
71. Eliza, M.Y.; Shahruddin, M.; Noormaziah, J.; Rosli, W.D.W. Carboxymethyl Cellulose (CMC) from oil palm empty fruit bunch (OPEFB) in the new solvent dimethyl sulfoxide (DMSO)/tetrabutylammonium fluoride (TBAF). *J. Phys. Conf. Ser.* **2015**, *622*, 12026. [CrossRef]
72. Zulkefli, S.; Abdulmalek, E.; Abdul Rahman, M.B. Pretreatment of oil palm trunk in deep eutectic solvent and optimization of enzymatic hydrolysis of pretreated oil palm trunk. *Renew. Energy* **2017**, *107*, 36–41. [CrossRef]
73. Hamzah, F.; Idris, A.; Shuan, T.K. Preliminary study on enzymatic hydrolysis of treated oil palm (Elaeis) empty fruit bunches fibre (EFB) by using combination of cellulase and β, 1-4 glucosidase. *Biomass Bioenergy* **2011**, *35*, 1055–1059. [CrossRef]
74. Abu Bakar, N.K.; Zanirun, Z.; Abd-Aziz, S.; Ghazali, F.M.; Hassan, M.A. Production of fermentable sugars from oil palm empty fruit bunch using crude cellulase cocktails with *Trichoderma asperellum* UPM1 and *Aspergillus fumigatus* UPM2 for bioethanol production. *BioResources* **2012**, *7*, 3627–3639.
75. Hossain, M.N.B.; Basu, J.K.; Mamun, M. The Production of Ethanol from Micro-Algae Spirulina. *Procedia Eng.* **2015**, *105*, 733–738. [CrossRef]
76. Yang, J.; Kim, J.E.; Kim, J.K.; Lee, S.H.; Yu, J.H.; Kim, K.H. Evaluation of commercial cellulase preparations for the efficient hydrolysis of hydrothermally pretreated empty fruit bunches. *BioResources* **2017**, *12*, 7834–7840. [CrossRef]
77. Bhatia, S.K.; Bhatia, R.K.; Choi, Y.K.; Kan, E.; Kim, Y.G.; Yang, Y.H. Biotechnological potential of microbial consortia and future perspectives. *Crit. Rev. Biotechnol.* **2018**, *38*, 1209–1229. [CrossRef]
78. Kusfanto, H.F.; Maggadani, B.P.; Suryadi, H. Fermentation of Bioethanol from the Biomass Hydrolyzate of Oil Palm Empty Fruit Bunch using selected yeast isolates. *Int. J. Appl. Pharm.* **2017**, *9*, 49–53. [CrossRef]
79. Nguyen, K.; Murray, S.; Lewis, J.A.; Kumar, P. Morphology, cell division, and viability of *Saccharomyces cerevisiae* at high hydrostatic pressure. *arXiv* **2017**, arXiv:170300547.
80. Evcan, E.; Tari, C. Production of bioethanol from apple pomace by using cocultures: Conversion of agro-industrial waste to value added product. *Energy* **2015**, *88*, 775–782. [CrossRef]
81. Ab Majid, A.H.; Zahran, Z.; Abd Rahim, A.H.; Ismail, N.A.; Abdul Rahman, W. Mohammad Zubairi, K.S.; Satho, T. Morphological and molecular characterization of fungus isolated from tropical bed bugs in Northern Peninsular Malaysia, *Cimex hemipterus* (Hemiptera: Cimicidae). *Asian Pac. J. Trop. Biomed.* **2015**, *5*, 707–713. [CrossRef]
82. Kannangara, S.; Dharmarathna, R.M.G.C.S. Jayarathna, D. Isolation, Identification and Characterization of *Trichoderma* Species as a Potential Biocontrol Agent against *Ceratocystis paradoxa*. *J. Agric. Sci.* **2017**, *12*, 51–62.
83. Shah, S.; Nasreen, S.; Sheikh, P. Cultural and Morphological Characterization of *Trichoderma* spp. Associated with Green Mold Disease of *Pleurotus* spp. in Kashmir. *Res. J. Microbiol.* **2012**, *7*, 139–144. [CrossRef]
84. Mustafa, A.; Khan, M.A.; Inam-ul-Haq, M.; Pervez, M.A.; Umar, U.D. Usefulness of Different culture media for in-vitro evaluation of *Trichoderma* spp. against seed borne fungi of economic importance. *J. Phytopathol.* **2009**, *21*, 83–88.
85. Prajankate, P.; Siwarasak, P. Co-culture of *Trichoderma reesei* RT-P1 with *Saccharomyces cerevisiae* RT-P2: Morphological Study. *Sci. Technol.* **2011**, *4*, 75–78.
86. De Azevedo, A.M.C.; De Marco, J.L.; Felix, C.R. Characterization of an amylase produced by a *Trichoderma harzianum* isolate with antagonistic activity against *Crinipellis perniciosa*, the causal agent of witches' broom of cocoa. *FEMS Microbiol. Lett.* **2000**, *188*, 171–175. [CrossRef]
87. Kumar, D.; Surya, K.; Verma, R. Bioethanol production from apple pomace using co-cultures with *Saccharomyces cerevisiae* in solid-state fermentation. *J. Microbiol. Biotechnol. Food Sci.* **2020**, *9*, 742–745. [CrossRef]
88. Aunsbjerg, S.D.; Andersen, K.R.; Knøchel, S. Real-time monitoring of fungal inhibition and morphological changes. *J. Microbiol. Methods* **2015**, *119*, 196–202. [CrossRef]

89. Alsuhaim, H.; Vojisavljevic, V.; Pirogova, E. Effects of Non-thermal Microwave Exposures on the Proliferation Rate of *Saccharomyces Cerevisiae* yeast. In Proceedings of the World Congress on Medical Physics and Biomedical Engineering, Beijing, China, 26–31 May 2012; pp. 1–5.
90. Jung, Y.H.; Kim, I.J.; Kim, H.K.; Kim, K.H. Dilute acid pretreatment of lignocellulose for whole slurry ethanol fermentation. *Bioresour. Technol.* **2013**, *132*, 109–114. [CrossRef]
91. Raman, J.K.; Gnansounou, E. Ethanol and lignin production from Brazilian empty fruit bunch biomass. *Bioresour. Technol.* **2014**, *172*, 241–248. [CrossRef]
92. Pandey, A.K.; Edgard, G.; Negi, S. Optimization of concomitant production of cellulase and xylanase from *Rhizopus oryzae* SN5 through EVOP-factorial design technique and application in Sorghum Stover based bioethanol production. *Renew Energy* **2016**, *98*, 51–56. [CrossRef]
93. Rajnish, K.N.; Samuel, M.S.; John, A.J.; Datta, S.; Chandrasekar, N.; Balaji, R.; Jose, S.; Selvarajan, E. Immobilization of cellulase enzymes on nano and micro-materials for breakdown of cellulose for biofuel production-a narrative review. *Int. J. Biol. Macromol.* **2021**, *182*, 1793–1802. [CrossRef] [PubMed]
94. Shokrkar, H.; Ebrahimi, S. Synergism of cellulases and amylolytic enzymes in the hydrolysis of microalgal carbohydrates. Biofuels. *Bioprod. Biorefining* **2018**, *12*, 749–755. [CrossRef]
95. Poornejad, N.; Karimi, K.; Behzad, T. Ionic Liquid Pretreatment of Rice Straw to Enhance Saccharification and Bioethanol Production. *J. Biomass Biofuel* **2014**, *1*, 8–15. [CrossRef]
96. Alam, M.Z.; Kabbashi, N.A.; Tompang, M.F. Development of single-step bioconversion process for bioethanol production by fungi and yeast using oil palm empty fruit bunches. In Proceedings of the 20th Symposium Malaysian Chememical Engineering, Kuala Lumpur, Malaysia, 19 December 2006; pp. 1–6.
97. Ferreira Filho, J.A.; Horta, M.A.C.; Beloti, L.L.; Dos Santos, C.A.; de Souza, A.P. Carbohydrate-active enzymes in *Trichoderma harzianum*: A bioinformatic analysis bioprospecting for key enzymes for the biofuels industry. *BMC Genom.* **2017**, *18*, 779. [CrossRef] [PubMed]
98. Wang, H.; Zhai, L.; Geng, A. Enhanced cellulase and reducing sugar production by a new mutant strain *Trichoderma harzianum* EUA20. *J. Biosci. Bioeng.* **2020**, *129*, 242–249. [CrossRef]
99. Qi, G.; Xiong, L.; Luo, M.; Huang, Q.; Huang, C.; Li, H.; Xuefang, C.; Xinde, C. Solvents production from cassava by co-culture of *Clostridium acetobutylicum* and *Saccharomyces cerevisiae*. *J. Environ. Chem. Eng.* **2018**, *6*, 128–133. [CrossRef]
100. Verma, G.; Nigam, P.; Singh, D.; Chaudhary, K. Bioconversion of starch to ethanol in a single-step process by coculture of amylolytic yeasts and *Saccharomyces cerevisiae* 21. *Bioresour. Technol.* **2000**, *72*, 261–266. [CrossRef]
101. Dey, P.; Rangarajan, V.; Nayak, J.; Bhusan, D.; Branden, S. An improved enzymatic pre-hydrolysis strategy for efficient bioconversion of industrial pulp and paper sludge waste to bioethanol using a semi-simultaneous saccharification and fermentation process. *Fuel* **2021**, *294*, 120581. [CrossRef]
102. Liu, Y.; Zhang, Y.; Xu, J.; Sun, Y.; Yuan, Z.; Xie, J. Consolidated bioprocess for bioethanol production with alkali-pretreated sugarcane bagasse. *Appl. Energy* **2015**, *157*, 517–522. [CrossRef]
103. Gonzales, R.R.; Kim, J.S.; Kim, S. Optimization of dilute acid and enzymatic hydrolysis for dark fermentative hydrogen production from the empty fruit bunch of oil palm. *Int. J. Hydrog. Energy* **2019**, *44*, 2191–2202. [CrossRef]
104. Zainan, N.H.; Alam, Z.; Al-khatib, M.F. Production of sugar by hydrolysis of empty fruit bunches using palm oil mill effluent (POME) based cellulases: Optimization study. *Afr. J. Biotechnol.* **2011**, *10*, 18722–18727.
105. Kamoldeen, A.A.; Keong, C.; Nadiah, W.; Abdullah, W.; Peng, C. Enhanced ethanol production from mild alkali-treated oil-palm empty fruit bunches via co-fermentation of glucose and xylose. *Renew. Energy* **2017**, *107*, 113–123. [CrossRef]
106. Syadiah, E.A.; Haditjaroko, L.; Syamsu, K. Bioprocess engineering of bioethanol production based on sweet sorghum bagasse by co-culture technique using *Trichoderma reesei* and *Saccharomyces cerevisiae*. *IOP Conf. Ser. Earth Environ. Sci.* **2018**, *209*, 12018. [CrossRef]
107. Jambo, S.A.; Abdulla, R.; Marbawi, H.; Gansau, J.A. Response surface optimization of bioethanol production from third generation feedstock—*Eucheuma cottonii*. *Renew. Energy* **2018**, *132*, 1–10. [CrossRef]
108. Khoja, A.H.; Ehsan, A.; Kashaf, Z.; Ansari, A.A.; Azra, N.; Muneeb, Q. Comparative study of bioethanol production from sugarcane molasses by using *Zymomonas mobilis* and *Saccharomyces cerevisiae*. *Afr. J. Biotechnol.* **2015**, *14*, 2455–2462.
109. Park, J.; Oh, B.; Seo, J.; Hong, W.K.; Yu, A.; Sohn, J.H.; Kim, C.H. Efficient Production of Ethanol from Empty Palm Fruit Bunch Fibers by Fed-Batch Simultaneous Saccharification and Fermentation Using *Saccharomyces cerevisiae*. *Appl. Biochem. Biotechnol.* **2013**, *170*, 1807–1814. [CrossRef] [PubMed]
110. Ahmad, F.U.; Bukar, A.; Usman, B. Production of bioethanol from rice husk using *Aspergillus niger* and *Trichoderma harzianum*. Bayero. *J. Pure Appl. Sci.* **2017**, *10*, 280.
111. Kassim, M.A.; Loh, S.K.; Bakar, N.A.; Aziz, A.A.; Mat Som, R. Bioethanol production from Enzymatically Saccharified Empty Fruit Bunches Hydrolysate using *Saccharomyces cerevisiae*. *Res. J. Env. Sci.* **2011**, *5*, 573.
112. Sahu, O. Appropriateness of rose (*Rosa hybrida*) for bioethanol conversion with enzymatic hydrolysis: Sustainable development on green fuel production. *Energy* **2021**, *232*, 120922. [CrossRef]
113. Ibrahim, M.; Abd-aziz, S.; Hassan, M.A. Oil Palm Empty Fruit Bunch as Alternative Substrate for Acetone—Butanol—Ethanol Production by *Clostridium butyricum* EB6. *Appl. Biochem. Biotechnol.* **2012**, *166*, 1615–1625. [CrossRef]

114. Alam, M.Z.; Al khatib, N.H.; Rashid, M.F. Optimization of bioethanol production from empty fruit bunches by co-culture of *Saccharomyces cerevisae* and *Aspergillus niger* using statistical experimental design. *J. Pure Appl. Microbiol.* **2014**, *8*, 731–740.
115. Anu; Singh, B.; Kumar, A. Process development for sodium carbonate pretreatment and enzymatic saccharification of rice straw for bioethanol production. *Biomass Bioenergy* **2020**, *138*, 105574. [CrossRef]
116. Chohan, N.A.; Aruwajoye, G.S.; Sewsynker-Sukai, Y.; Gueguim Kana, E.B. Valorisation of potato peel wastes for bioethanol production using simultaneous saccharification and fermentation: Process optimization and kinetic assessment. *Renew. Energy* **2019**, *146*, 1031–1040. [CrossRef]
117. Ansar; Nazaruddin; Azis, A.D.; Fudholi, A. Enhancement of bioethanol production from palm sap (*Arenga pinnata* (Wurmb) Merr) through optimization of *Saccharomyces cerevisiae* as an inoculum. *J. Mater. Res. Technol.* **2021**, *14*, 548–554. [CrossRef]
118. de Albuquerque Wanderley, A.C.; Soares, M.L.; Gouveia, E.R. Selection of inoculum size and *Saccharomyces cerevisiae* strain for ethanol production in simultaneous saccharification and fermentation (SSF) of sugar cane bagasse. *Afr. J Biotechnol* **2014**, *13*, 2762–2765.
119. Neelakandan, T.; Usharani, G.; Nagar, A. Optimization and Production of Bioethanol from Cashew Apple Juice Using Immobilized Yeast Cells by *Saccharomyces cerevisiae*. *Am. J. Sci. Res.* **2009**, *4*, 85–88.